Scuola Internazionale Superiore di Studi Avanzati - Trieste

Identifying molecular determinants of prion conversion

Kate Pischke

A thesis submitted for the degree of
Doctor of Philosophy
in Functional and Structural Genomics
October 2017

SISSA - Via Bonomea 265 - 34136 TRIESTE - ITALY

Scuola Internazionale Superiore di Studi Avanzati

Area of Neuroscience
Ph.D. in Structural and Functional Genomics

Identifying molecular determinants of prion conversion

Candidate
Kate Elizabeth Pischke

Supervisor
Prof. Giuseppe Legname

Thesis submitted in partial fulfillment of the requirements
for the degree of Doctor Philosophiae Academic Year 2016/2017

Abstract

Prion diseases have been widely studied, but despite many great leaps in our knowledge of prion and protein misfolding diseases in general, many gaps remain. One example is the structural triggers or provocators of prion conversion found within the prion protein (PrP) itself. While factors interacting on PrP can promote or dissuade conversion, it is also evident that inherent properties of differing PrP (presumably especially conformation) have an effect on the likelihood of prion conversion. Previous work from our lab found that the substitution of histidine 95 with a tyrosine increased prion conversion, while the same individual substitution at four other copper-binding histidines of PrP had no effect on prion conversion propensity. Therefore, we focused on the role of mutations at this amino acid of the mouse PrP (MoPrP), H95, to explore if this increase in prion conversion is unique to the H95Y mutation and better understand how mutations here affect conversion. In this original work, we perform an amino acid scan at H95, replacing the histidine with every other common amino acid and comparing the prion conversion propensity. The results are remarkable with the residues with hydrophobic side chains increasing prion conversion by about 150% and residues with electrically-charged side chains decreasing prion conversion by about 75%, both compared to WT PrP. We continued and provide the first robust data that mutations on the prion protein at residue 95 (specifically H95D, H95E, H95K and H95R) decrease the propensity for cellular PrP (PrP^{C}) to misfold into scrapie PrP (PrP^{Sc}), with transient transfection of mutant proteins into ScN2a cells. We next biochemically characterize PrP H95E and PrP H95Y, the most promising mutant for reducing and increasing conversion, respectively, in N2aPrP$-/-$ cells stably transfected with the mutant PrPs. We conclude that PrP H95E and PrP H95Y are biochemically similar to PrP WT. Also with these generated stable cell lines, we use immunofluorescence to study the localization and trafficking of the mutant PrPs relative to organelle markers. The only difference we observed was relative to the endosomal recycling compartments, with PrP H95E co-localizing less compared to PrP WT and PrP H95Y co-localizing more compared to PrP WT. This is in agreement with other work that links the endosomal recycling compartments with prion conversion. More work is required to understand what structural changes, if any, occur on the PrP H95E mutant and to understand if this plays a role in conversion, similar to the work carried out on the PrP H95Y mutant. At this point we conclude that the replacement of PrP H95 with electrically charged side chains decreases the prion conversion propensity, and after a detailed study of PrP H95E conclude that this is likely due to reduced co-localization with the endosomal recycling compartments, but we cannot rule out the influence of structural changes and would like to continue studies along this line.

Contents

List of Figures

List of Tables

Chapter 1
1 Introduction

Prion diseases have been widely studied, but despite many great leaps in our knowledge of prion diseases and protein misfolding diseases in general, many gaps remain. One example is the structural triggers or provocators of prion conversion found within the prion protein (PrP) itself. While it is true that many factors interacting on/with PrP can promote or dissuade conversion, it is also evident that inherent properties of PrP (presumably especially conformation) have an effect on the likelihood of prion conversion. To better understand this, we have focused on a single amino acid of the mouse PrP (MoPrP): H95, which, amazingly, simply by its substitution with other single amino acids can dramatically change the prion conversion propensity of PrP. In this original work, which I present here, we provide the first robust data that the mutation PrP H95E results in diminished prion conversion and link this to the mutated protein's diminished accumulation in the endosomal recycling compartment *in vitro*.

A note on terminology: many terms have been suggested in the literature to refer to the prion protein, for simplicity in this dissertation I will use PrP to refer to the prion protein in general, PrP^{C} in reference specifically to the cellular prion protein and PrP^{Sc} or prion to broadly refer to the misfolded form of the prion protein associated with disease. Also, for the numbering of the prion protein I will use as my reference the mouse Prnp codon numbering, which is -1 compared to human PRNP due to a single amino acid deletion in the N-terminus (Gly54), unless indicated otherwise.

1.1 Prion Diseases

Incurable, irreversible, fatal, and rare: prion diseases are a group of neurodegenerative disorders affecting humans and other mammals. Their uniqueness relies on a surprising phenomena: the ability to infect and replicate without nucleic acids. It took decades of research and head-scratching to alter the standard views shared by the scientific community with respect to the characterization of infection, that nucleic acids are necessary to replicate. While nucleic acids are commonly needed (in viral and bacterial infections for example), prion diseases replicate using only the information stored in the protein conformation [31].

Prion diseases manifest as genetic, sporadic or infectious [15]. They include Creutzfeldt-Jakob disease (CJD), Variant Creutzfeldt-Jakob Disease (vCJD), Gerstmann-Straussler-Scheinker Syndrome and Fatal Familial Insomnia in humans; Bovine Spongiform Encephalopathy in cattle, Chronic Wasting Disease in cervids, and scrapie in sheep, to name a few (for a more complete review see [8]). Classic neuropathological features of prion disease are spongiform change, neuronal loss and gliosis (of astroglia and microglia) [7]. Clinical symptoms and incubation times vary widely, but generally once clinical symptoms; including most frequently motor dysfunction, cognitive impairment and cerebellar dysfunction; appear disease progression is rapid, leading to death.

Premortem diagnosis is difficult and there is currently no standard clinical diagnostic test. However, studies with real-time quaking-induced conversion (RT-QuIC), which detects prions by amplifying them into amyloid fibrils, has shown promise as a tool for diagnosis, especially from olfactory mucosal brushings [12]. All treatments to date have failed to modify disease outcome [8].

Research in the prion field endeavours, ultimately, to find treatments for prion diseases, a branch of infectious diseases whose mechanisms and effects have perplexed the scientific community for decades on end. The understanding of the PrP structure, mainly how changes in the primary structure of PrP affect the likelihood for prion conversion, is a stepping stone toward this endeavour and encompasses some of the most exciting venues in prion research. Why does a simple, at first sight, conformational change produce such extreme and devastating effects in living organisms? The understanding of the mechanisms involved will shed light in what has become an endless fight against neurodegenerative diseases. A fight which will only be won by unveiling the long-sought-after prion switch, critical for disease onset and propagation.

1.2 The prion protein (PrP)

PrP is highly conserved among mammals [9]. PrP is expressed in both the nervous system and peripheral tissues, however its highest expression levels occur in neuronal cells [13].

1.2.1 Cellular prion protein (PrP^C) structure

Cellular prion protein (PrP^C), refers to the physiological, native folded form of PrP. PrP^C is predominantly found attached via a Glycosylphosphatidylinositol (GPI) anchor to the outer leaflet of the plasma membrane, exposed to the extracellular space. The C-terminal of PrP^C (127-231) is a structured, globular and largely α-helical, with three

α-helices (α1, α2, α3) and two short β-strands (β1, β2). The N-terminal domain (23-126) is intrinsically disordered and contains: two charged clusters (CC1 and CC2), the octarepeat region (OR; 59-90), the non-octarepeat region (non-OR; 91-110) and a hydrophobic domain (HD; 111-126). The N-terminal can bind copper (Cu^{2+}) with high affinity at four sites in the OR region and two sites in the adjacent non-OR region. Additionally, a disulphide bridge and two N-glycosylation sites are found in the globular domain (Figure 1.1) [69] [73].

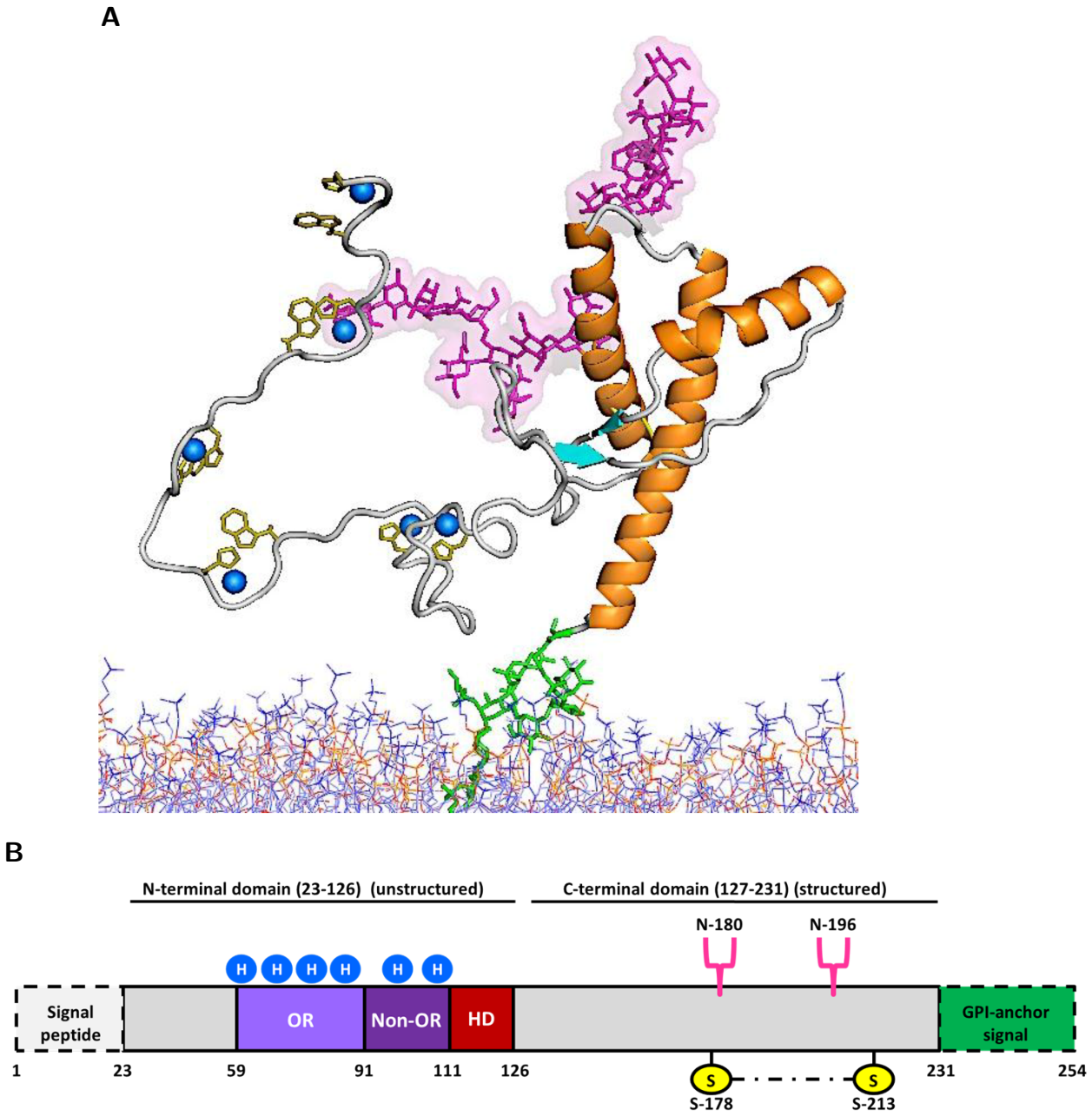

Figure 1.1: PrP^C Structure (**A**) Schematic diagram of PrP^C structure. The carbohydrate moieties are shown in pink, the C-terminal GPI-anchor in green extending into the cell membrane and the drawn residues in the N-terminal domain are known to bind copper ions (blue spheres). (**B**) Organization of mouse PrP. Unprocessed PrP includes the signal peptide (1-22), octarepeat region (OR; 59-90), non-octarepeat region (non-OR; 91-110), hydrophobic domain (HD; 111-126), one disulphide bond between cysteine residues (178-213), two N-linked glycosylation sites (at residues 180 and 196), and a GPI-anchor attached to the C-terminus of PrP replacing the GPI-anchor signal (residues 232 to 254). The six histidines of the N-terminal available to bind copper are shown in blue circles. GPI: glycophosphatidylinositol. Modified from [10].

1.2.2 Biogenesis of PrP^C through the secretory pathway

PrP^C is translated and undergoes several post-translational modifications on its way to expression on the cell membrane. First, ribosomes began translation of Prnp mRNA in the cytosol, until the signal peptide (1-22) directs it to be co-translationally translocated to the endoplasmic reticulum (ER) [123]. Here, the remainder of the protein is translated directly into the ER. During translation, N-linked oligosaccharide chains can be added at neither, one, or two of the available asparagine residues, 180 and 196 (this corresponds to the non-, mono- or diglycosylated forms of PrP, respectively). The N-linked oligosaccharide chains at this point are the high mannose type and are sensitive to digestion by Endoglycosidase H (Endo H), therefore PrP^C at this stage is considered immature. The hydrophobic C-terminal α-helix, a GPI-signal peptide, is left buried in the membrane of the ER after translation and the signal peptide is cleaved, leaving 23-254. The GPI-signal peptide is also cleaved and replaced with a GPI anchor, which stays inserted in the membrane, now leaving 23-231 [117] [118]. The oxidative environment of the ER lumen allows for the formation of the disulphide bond between cysteine residues 178 and 213 [122].

Next, PrP^C is transported by vesicles to the Golgi. Here the N-linked oligosaccharide chains are modified, resulting in diverse and complex-type chains containing sialic acid, rendering them resistant to Endo H digestion, but still susceptible to digestion by the Peptide:N-Glycosidase F (PNGase F) [124]. PrP^C is now considered mature and is transported to the cell surface by an exocytic vesicle. Here it remains anchored, by the GPI, to the outer leaflet of the plasma membrane [119]. At the cell surface PrP^C associates with cholesterol- and glycosphingolipid-rich lipid rafts through its GPI anchor [14].

1.2.3 PrP trafficking and processing

From the cell membrane, PrP can enter into the endocytic pathway. In neurons, PrP^C translocates out of lipid rafts into detergent-soluble regions where it undergoes endocytosis in clathrin-dependent pathways. Copper binding to PrP^C promotes its endocytosis via the clathrin-dependent pathway [99] [83]. PrP^C then enters early endosomes and is sorted to the endosomal recycling compartment and returned to the plasma membrane, the most common route for PrP^C, or to late endosomes/lysosomes for degradation [120] [121] (Figure 1.2).

Additionally in the endocytic compartments, a fraction of PrP is proteolytically cleaved through PrP processing. Mature PrP proteolytic cleavage is termed α-, β- and possibly a third type, γ-cleavage. PrP cleavage creates the PrP fragments: N1 and C1, N2

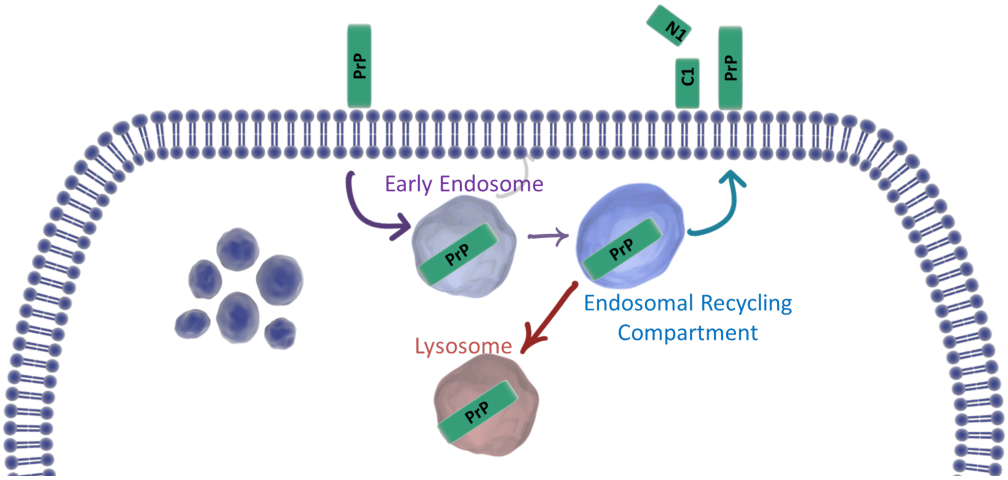

Figure 1.2: Schematic of the route commonly followed by PrP in the endocytic pathway.

and C2, and C3, respectively. Studies indicate that PrP cleavage may have important physiological and pathological implications [20] [21] [22] [23], which we will discuss in more detail in Section 1.3.2.3.

1.2.4 PrP^C and copper binding

1.2.4.1 Copper and PrP^C expression

First it was found that copper, when added extracellularly to *in vitro* neuronal cultures significantly decreases PrP^C mRNA, increases the release of PrP^C into the culture medium and decreases the total PrP^C protein present in the cells [92]. Treatment with cuprizone (CPZ), a well known selective copper chelator that does not affect cell viability and cannot cross plasma membranes, completely restored PrP^C mRNA and protein expression. However, other studies found the opposite, that adding copper to cell lines results in increased levels of PrP^C expression [98] and that primary neurons exposed to increased copper concentrations also upregulated PrP expression at both the mRNA and protein levels (copper chelation, this time by bathocuprionedisulfate (BCS), inhibited the increase of PrP^C expression) [93].

1.2.4.2 Endocytosis of PrP^C and copper uptake

PrP^C predominantly localizes at synaptic membranes, especially presynaptically, where copper is also highly localized [94]. It has been shown that PrP^C expression influences brain copper content. When PrP^C is removed in Tg mice, referred to as PrP knockout mice (PrP KO mice), these mice showed a synaptosomal copper decrease of more than 50% compared to WT mice [97] [95]. Copper also influences PrP^C endocytosis, copper

added to the medium of cultured neuroblastoma cells rapidly and reversibly stimulates the endocytosis of PrP^C from the cell surface [99]. Additionally, deletion of the one of the copper-binding regions, the OR, stopped the endocytosis, indicating that this region directs the internalization of PrP^C in response to copper. Interestingly, a mutant form of PrP with nine additional octarepeats, which is associated with familial prion disease, was unable to participate in copper-mediated endocytosis [83]. These results suggest a physiologically relevant role for PrP^C binding with copper, where PrP^C could serve as a copper transport mechanism across the membrane or a type of copper buffer at the synaptic cleft.

1.2.5 PrP^C Function

The fact that PrP^C is highly evolutionarily conserved among mammals suggests that it carries out some beneficial physiological functions, or evolutionary selection would likely have eliminated it. PrP^C is expressed in many organs and tissues, with the highest levels of expression being the central and peripheral nervous systems (CNS and PNS) [26]. Increasing evidence supports a central role for PrP^C in neuroprotection. Proposed PrP^C functions include synaptic plasticity [74], cell signaling [76], neuronal growth and differentiation [75], N-methyl-D-aspartate (NMDA) receptors modulation [77] [111] [79] and brain metal homeostasis [80]. These latter two proposed functions directly involve the ability of PrP^C to bind divalent cations, primarily copper [81].

Gross phenotypes are not observed in PrP KO mice [27]. However, upon careful and detailed studies structural and functional abnormalities in the PNS as well as structural and functional abnormalities following the application of stressors in the CNS are observed.

A plethora of phenotypes have been attributed to the PrP KO mice, but researchers have realized that some of these were simply genetic artifacts of the underlying mouse models [19]. Many experiments are being reassessed using new animal models created with the latest advancements in gene editing technology, most notably, the strictly co-isogenic C57BL/6 J-Prnp ZH3/ZH3 mice from the Aguzzi lab, which differ from wild-type mice only by eight deleted nucleotides in the Prnp reading frame [27]. Many physiological roles of PrP^C have been put forward, most of which focus on the unstructured N-terminal as the primary site involved in the function. Proposed functions for PrP^C relevant to this work will be discussed. For an in-depth review see [19].

1.2.5.1 The functional N-terminal of PrP^C

PrP^C can bind to divalent cations such as copper and zinc via the OR and non-OR regions of the flexible N-terminal [51]. The PrP^C N-terminal has been reported to interact with a substantial number of different proteins and that these interactions constitute a physiological function of PrP^C. In this manner, PrP^C has been implicated in many cellular process [19]. However, it is important to keep in mind that these interactions may also be a natural consequence of the unstructured conformation of the N-terminal region of PrP^C. Therefore, studies simply showing interaction, without strong supporting evidence on functionality should be taken with a grain of salt as their only scientific conclusion pertains to what basically amounts to chemical properties.

The N-terminal of PrP^C (residues 23-126) is unstructured in solution [68], but it is generally divided up into three regions of interest: the octarepeat (OR), the non-octarepeat (non-OR) and the hydrophobic domain (HD).

The OR region, residues 59-90, is composed of four tandem repeats of eight amino acids (PHGGGWGQ), with histidine as the primary residue involved in copper coordination [65] [66]. This region can coordinate up to four copper ions, with distinct coordination geometries and high affinity [70]. The OR is very well conserved, suggesting a functionally significant role for the region [67]. Copper can also bind to PrP outside of the OR region, in the neighboring non-OR region (residues 91-110), at H95 and H110 [71]. Next in line is the HD (residues 111-126), which has been reported to play a role during prion conversion [72]. These latter two regions, spanning residues 91-126, also show a high degree of conservation among mammalian species [73].

1.2.5.2 N-methyl-D-aspartate receptor (NMDAR) modulation by PrP

Several studies have suggested PrP^C involvement in synaptic mechanisms and protection against neuronal excitotoxicity at the molecular level. Documented interaction of PrP^C with ion channels and metabotropic glutamate receptors may provide insights into potential mechanisms.

We will look into more detail into the interaction of PrP^C with the glutamate receptor and ion channel, N-methyl-D-aspartate receptors (NMDAR). NMDAR are heterotetramers composed of two GluN1 and two GluN2 subunits and mediate critical CNS functions, though excessive NMDAR activity can cause neuronal damage [110]. PrP^C was found to inhibit NMDAR and prevent calcium influx, which in excess is excitotoxic, by association with the GluN2D subunit of the receptor [111]. Hippocampal neurons isolated from PrP KO mice exhibited enhanced and prolonged NMDAR-evoked currents, due to a functional upregulation of NMDAR with GluN2D subunits and NMDAR overactivity

resulted in an increase of neuronal excitability. These effects were rescued upon the overexpression of exogenous PrP^C and phenocopied by PrP^C RNA interference. PrP KO mice were also shown to have increased depressive-like behaviour [112] and a reduced pain threshold [113], with both behaviours reversed by pharmacological inhibition of NMDAR. These studies suggest a functional role for PrP that is linked to NMDAR regulation in neurons, restraining overactivity, with behavioural consequences.

Work continued on PrP and NMDAR and it was found that the interaction between PrP^C and NMDAR is copper-dependent [114]. When copper is chelated from cultured rodent hippocampal neurons a similar effect is seen as when PrP^C is ablated, NMDAR show non-desensitizing currents even at physiologically low glycine concentrations. This suggests that PrP^C interacts in a copper-dependent manner with the NMDAR, where copper-bound PrP^C acts to limit excessive NMDAR activity that could lead to neuronal damage. This work was expanded upon by another group, who also showed that PrP^C and copper cooperatively inhibit NMDAR, adding that the precise mechanism is S-nitrosylation, a post-translational protein modification resulting from the chemical reaction of nitric oxide with cysteine residues, of NMDAR [115]. They found that NMDAR S-nitrosylation was decreased in PrP KO compared to wild type (WT) mice and that copper chelation decreased NMDAR S-nitrosylation in WT but not PrP KO mice. They propose that PrP^C-bound copper ions act as electron acceptors in the reaction between nitric oxide and NMDAR cysteine thiols, thereby supporting NMDAR S-Nitrosylation, which is neuroprotective to the cell by reducing NMDAR overactivation.

1.3 The pathological form of the prion protein (PrP^{Sc})

PrP scrapie (PrP^{Sc}) is the disease causing form of the prion protein. PrP^{Sc} has the same amino acid sequence as PrP^C, but its tertiary structure is altered. This change in conformation by misfolding is termed conversion, a post-translational event where PrP^C misfolds into PrP^{Sc}. This conversion is followed by self-propagation, spreading, and accumulation of PrP^{Sc}, often resulting in disease.

Evidence suggests that PrP^C can convert into diverse self-propagating conformations of PrP^{Sc}, each of which in turn can propagate its own tertiary structure often with distinctive biochemical and histopathological signatures [16]. This phenomena is termed prion strains [17]. PrP^{Sc} is classically defined as detergent insoluble and protease resistant [18], but it has now been well documented that prion infectivity can occur even in strains that are sensitive to protease digestion [136] [137] [138].

1.3.1 The protein-only hypothesis

Central to the prion field is the protein-only hypothesis. This states that the main (and perhaps the sole) infectious agent of prion diseases is a misfolded protein, which carries the information in its tertiary structure [32] [31]. Evidence collected to date overwhelmingly supports the protein-only hypothesis. Critical landmarks are discussed briefly in this section (for a detailed review see [33]).

Some of the first evidence supporting this hypothesis was the fact that PrP KO mice are completely resistant to prion disease. PrP KO mice are incapable of propagating PrP^{Sc} and do not become ill. So, it was shown that PrP is required for prion replication and disease progression [116].

The absolute evidence for the protein-only hypothesis was the production of infectious material from pure WT PrP. To this aim in 2004, bacterially expressed recombinant prion protein (rPrP) was induced to misfold and aggregate *in vitro*, then injected into Tg mice overexpressing PrP [34]. These mice succumbed to a transmissible neurodegenerative disease with a long incubation period. Another group achieved the same results after serial passages using another method to misfold and aggregate rPrP, but importantly in WT animals (this time Syrian hamsters) [35]. These, and numerous other experiments to date, notably using PMCA, provide extremely strong evidence for the prion protein as the main infectious component of prion disease. However, despite infection achieved in these cases, there was an unusually long incubation period and often an imperfect attack rate [36]. Then, *de novo* generation of bona fide infectious prions *in vitro* by PMCA that cause classic prion disease in WT hamsters was reported, where mixing rPrP with phospholipids and RNA was the crucial step to achieve increased infectivity [37]. It seems that efficient PrP^{C} conversion to highly infectious PrP^{Sc} is aided by the presence of host-encoded molecules, but it is not obligatory for the production of infectious PrP^{Sc} [33].

All in all, the numerous experiments producing synthetic infectious prions *in vitro* by various methods support the protein-only hypothesis of prions. Moreover, the research lines proposing that several other proteins transmit biological information in a prion-like manner, has reinforced the prion hypothesis. To name a few: in humans many neurodegenerative diseases involve self-replicating proteins, referred to as protein misfolding disorders (PMD), amyloid-β [39], α-synuclein [40], tau protein [38] (studies suggesting the existence of distinct strains of these proteins, though without infectivity, has also strengthened the prion hypothesis [43] [43]); and in yeast several prion-like proteins carrying out functional biological roles such as new metabolic phenotypes have been studied [41]. The protein-only phenomenon therefore potentially has widespread implications.

1.3.2 PrP^{Sc} and prion disease

1.3.2.1 PrP^{Sc} structure

Common structural features shared among PrP^{Sc} include an increase in the proportion of β-sheet motifs, the ability to form aggregates, insolubility and often resistance to proteinase digestion. In contrast, PrP^{C} is soluble, low in β-sheet content and highly susceptible to proteinase digestion [139].

PrP^{Sc} that is resistant to proteinase digestion can be detected by proteinase K (PK) digestion, resulting in the N-terminal truncation leaving a PK-resistant core of about 142 amino acids, referred to as PrP27-30, in reference to its apparent mass of 27-30 kDa after electrophoresis. Not all PrP^{Sc} of prion diseases is resistant to protease digestion [56]. The secondary structure can also be used to distinguish between PrP^{C} and PrP^{Sc}. Fourier Transform Infrared Spectroscopy (FTIR) and circular dichroism (CD) studies have shown that unlike PrP^{C}, which is predominantly α-helix (47% α-helix and only 3% β-sheet), PrP^{Sc} is β-sheet enriched (43% β-sheet and 30% α-helix) [57].

The most recent studies on PrP^{Sc} structure using X-ray fiber diffraction [59] and electron cryomicroscopy [58], point to a four-rung β-solenoid structure as a key feature for the architecture of GPI-anchorless PrP 27-30 mammalian prions. This puts important restrictions on the templating mechanisms involved and future studies will undoubtedly shed more light on this area.

1.3.2.2 PrP^{Sc} conversion

Two main models have been proposed for the PrP^{C} to PrP^{Sc} conversion process. The "template directed-refolding model" proposes a heterodimeric interaction between PrP^{C} and PrP^{Sc} monomers, where PrP^{C} overcomes the kinetic barrier and forms a new PrP^{Sc} molecule. This interaction then dissolves and the two monomers of PrP^{Sc} are released, each of which can bind to and convert other PrP^{C} substrate [61] [62]. However, this model is inconsistent with mathematical models of prion infectivity [125] [126]. Instead, these models indicate that small oligomers would act as the most infectious prion units.

Studies support a minimum infectious unit of at least 5 PrP units, with the highest infectivity in the 14-28 monomer range [126] [127]. This is in support of the "nucleation-dependant polymerization model", which proposes that PrP^{C} and PrP^{Sc} monomers are in a reversible thermodynamic equilibrium that strongly favors PrP^{C}. However, if the critical event of a primary nucleation event of an oligomeric PrP^{Sc} seed is able to form, this structure is stable and can be infectious [63] [64]. The seed promotes the self-templated conversion of soluble monomer PrP^{C} at the ends of the oligomer

seed, growing into a fibril [128]. The number of templating surfaces (i.e. the free ends of the fibrils) is a limiting factor for the rate of conversion and consequently disease progression. More templating sites are thought to be produced by secondary nucleation processes, such as fragmentation [60].

PrP can be converted *in vitro* into oligomers and fibrils fairly easily. However, these oligomers are often not toxic to cells, and even more challenging has been to produce *in vitro* oligomers with infectivity titers seen in bona fide prions [44]. This and other work, points to a disconnect between prion replication, toxicity and infectivity. For example, PrP KO cells show no signs of toxicity even when bona fide prions accumulate at high levels [45]. In this experiment, PrP^{C}-expressing neural tissue grafted into PrP KO brains exhibit scrapie pathology, but not the neighboring PrP KO tissue despite the presence scrapie fibrils and plaques.

Another process to consider is cell-to-cell spread of prions. Large cargo classically enters into cells by receptor-mediated endocytosis [46]. PrP^{C} can undergo clathrin-mediated endocytosis to early endosomes and is then sorted to endosomal recycling compartment, which reroute PrP^{C} back to the plasma membrane, or to late endosomes/lysosomes for degradation. It is difficult to distinguish the exact compartments in which prion replication occurs due mainly to the difficulty discerning PrP^{C} from PrP^{Sc} in situ, however many studies suggest that it occurs throughout the endocytic pathway [47] [49] and/or at the plasma membrane [48].

Specifically within the endocytic pathway, the endosomal recycling compartment (ERC) was found to be important for prion conversion [129]. Here the levels of PrP^{Sc} generated in chronically infected neuronal cell lines were analyzed under conditions where intracellular trafficking was selectively impaired. When PrP was blocked from exiting the early endosomes, PrP^{Sc} levels were diminished, indicating that the sorting from the early endosomes to subsequent compartments was essential for efficient prion conversion. PrP can be trafficked from early endosomes to late endosomes or to the ERC. Decreasing the number of late endosomes did not diminish PrP^{Sc} formation. However, when PrP sorting from early endosomes to the ERC is specifically impaired, PrP^{Sc} levels are drastically reduced. Furthermore, when PrP exit from the ERC is impaired, PrP^{Sc} levels increase. This sets forth firm evidence that PrP accumulation in the ERC promotes PrP^{Sc} production. Additionally, another study of the subcellular distribution of PrP^{Sc} in scrapie-infected mouse hippocampal sections found a large increase of PrP^{Sc} in the endosomal recycling compartments, also suggesting this as a possible conversion site [130].

Surprisingly, PrP^{Sc} is still formed and internalized in cells when the dynamin/clathrin-dependent endocytosis and macropinocytosis pathways are inhibited [50]. This suggests these pathways are either not involved in PrP^{Sc} formation and internalization or that

the process can occur through multiple pathways. Prion conversion is also diminished by the disruption of lipid raft integrity, where PrP^C associates at the cell membrane.

1.3.2.3 PrP cleavage role in prion disease

While PrP is cycling through the endocytic compartments it can be proteolytically cleaved. The type of cleavage PrP undergoes, if any, impacts the ability of the resulting fragments to participate in subsequent conversion events (Figure 1.3).

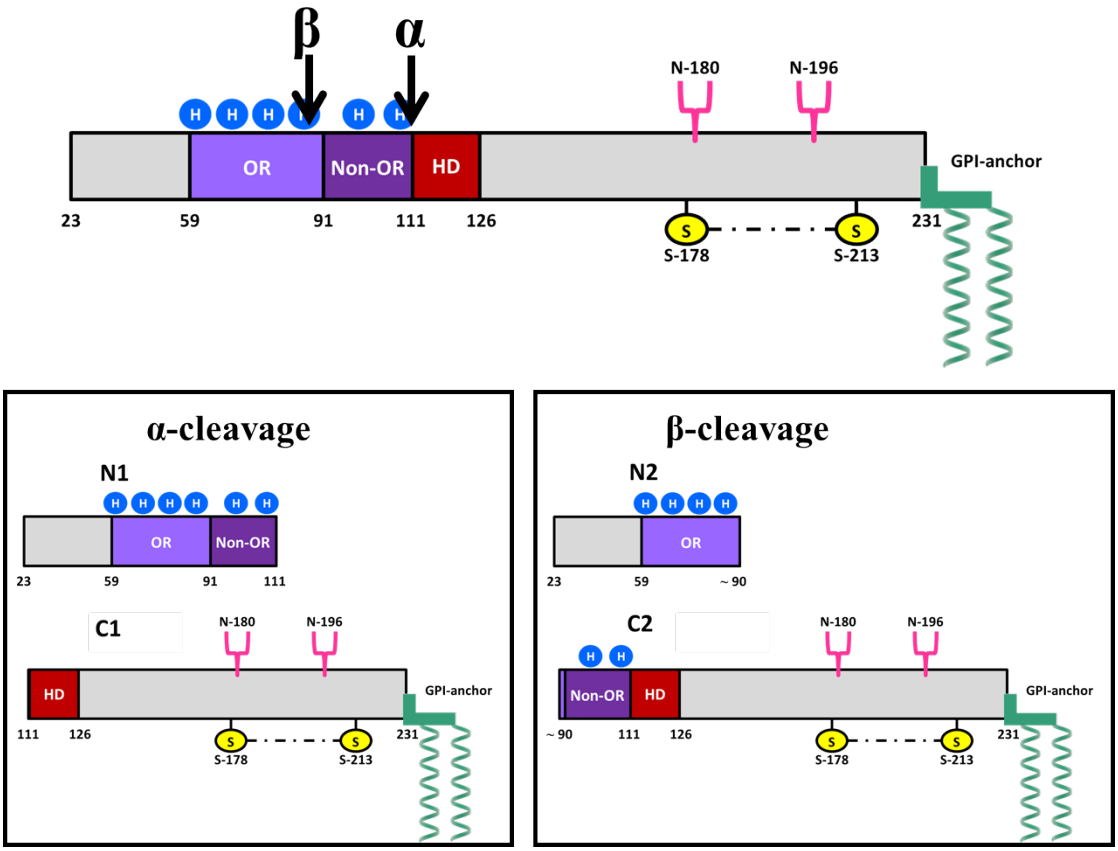

Figure 1.3: Schematic diagram of PrP processing. Modified from [11].

First we will look in more detail at α-cleavage. The membrane-anchored C1 fragment, a product of α-cleavage between residues 110/111 or 111/112, is the major proteolytic fragment of PrP^C [131]. α-cleavage divides PrP right between the non-OR and hydrophobic domain regions, a key area for prion conversion. Indeed, it has been shown [24] that transgenic (Tg) mice expressing only the C1 fragment of PrP (PrP(Δ23-111)), termed Tg(C1), show no spontaneous disease and these mice, when inoculated with scrapie prions do not accumulate PrP^{Sc} nor succumb to prion disease. This strongly suggests that C1 cannot convert into PrP^{Sc}. If Tg(C1) mice co-express C1 and WT PrP, they do get sick after scrapie prion inoculation, but at a much later date than

WT mice. The authors conclude that the C1 fragment acts as a dominant-negative inhibitor of PrP^{Sc} formation.

Other studies show that Tg mice lacking the α-cleavage site of PrP have spontaneous neurodegeneration, though pathologically distinct from prion diseases (for a review see [25]). This suggests that the production of the C1 and N1 fragment play an important role in the brain apart from resisting PrP^{Sc} conversion.

β-cleavage occurs upstream of the α-cleavage site at roughly the end of the OR region ($\sim$residue 90), producing the N2 and C2 fragments [131]. Under physiological conditions β-cleavage occurs at low levels compared to α-cleavage. However, during prion disease β-cleavage is more prevalent, with C2 fragments found at high levels in the brains of CJD patients [22]. Digestion by proteinase K (PK) results in a fragment comparable to C2 and PrP^{Sc} processed by PK or β-cleavage retains its infectivity; importantly, in both cases the non-OR and hydrophobic domain region remains intact. This was also seen *in vivo* with Tg mice expressing an equivalent to the C2 fragment (Δ32-80) had no spontaneous phenotype, but were susceptible to prion infection with incubation times similar to mice expressing WT PrP [84].

From studies on α- and β-cleavage of PrP, a necessity for prion conversion of PrP is an intact non-OR and hydrophobic domain regions. This region is destroyed by α-cleavage and the resulting C1 fragments are resistant to conversion into PrP^{Sc}. In contrast, β-cleavage (and similarly PK digestion) leaves this non-OR, hydrophobic domain region intact and will convert into PrP^{Sc}. These key regions, residues 90-126, of PrP conversion have important implications for furthering our understanding of the conversion process.

1.3.2.4 Deletions and insertions of the N-terminal and disease

In vivo studies also have shown that residues 90-126 are involved in prion generation and maintaining physiological PrP^{C} function(s). Deletion of only residues within the OR region (PrPΔC; Δ32-93), results in mice that do not display any pathological phenotype [90] and are susceptible to prion infection, but with long incubation times [105]. Extended deletions, however, which include the OR, non-OR and HD (PrPΔE, Δ32-121; PrPΔF, Δ32-134) induce pathological lesions and result in death at 3-4 months [88]. The expression of PrP with deletions only of the non-OR and HD (PrPΔCD; Δ94-134) induces a rapidly progressive, lethal phenotype with extensive central and peripheral myelin degeneration. Finally, a PrP variant lacking only 8 residues (PrPΔpHC; Δ114-121), which is a large segment of the HD, was innocuous. Another group also found that mice expressing PrP Δ105-125 (deleting one of the two non-OR

copper binding sites and the entire HD), develop a severe neurodegenerative illness that was lethal within 1 week after birth [89].

Naturally occurring missense mutations clustered in the non-OR region and within the palindromic motif (P102L, P105L, G114V and A117V, human numbering) result in GSS syndrome [140]. GSS syndrome is characterized by PrP^{Sc} amyloid plaque deposits in the brain. These PrP^{Sc}-inducing mutations support the idea of the non-OR as a key influencer of PrP^{C} function and prion conversion.

1.3.2.5 Large population analysis of the prion protein gene and the identification of a spontaneous PrP H96Y mutation in a patient

A large set of human genomic data has been studied to assess the risk of prion disease in relation to variants in the prion protein gene (PRNP) [28]. The results challenge many missense PRNP variants that have been reported as pathogenic in the literature. Most are likely benign PRNP variants falsely assigned as pathogenic, but some do confer disease susceptibility but with vastly ranging penetrance. Interestingly, three heterozygous loss-of-function variants were identified in healthy older individuals. So it seems heterozygous loss of PRNP in humans is tolerated and could represent an avenue for prion disease therapy. Most interestingly for our current work, they list a rare PRNP variant, H96Y (human numbering, mouse numbering equivalent: H95Y), as a probable prion disease case from Spain [28].

1.3.2.6 Prion diseases and copper

Copper's effect on the prion protein, function and possible link with prion diseases includes many contradicting studies have been reported concerning the involvement of copper in prion diseases, making it very difficult to understand the true relationship between copper and PrP. It is likely that these contradictions arise because of the complicated nature of copper and PrP. Or an intricate balance where differences of the cell or animal model and/or experimental methods, even small, could propagate to a large differences in the final outcome.

In vivo studies reported that the addition of dietary copper to scrapie-infected animals significantly delayed prion disease onset [103] [104]. Inconsistently, other *in vivo* studies reported the opposite. One early study found that cuprizone, a copper chelator, could delay or prevent terminal illness in scrapie-infected mice, though with very low inoculation titers and low reproducibility [100]. Another study using D-(-)-penicillamine (D-PEN) as a copper chelator, also found delayed disease onset in scrapie-infected mice [109]. Of course, these *in vivo* studies involve changing copper homeostasis, a

delicate balance, on a whole-animal level and it may simply be that copper influence on PrP^C and PrP^{Sc} is too intricate to be reproducibly studied in such broad-stroke experiments.

Addition of copper inhibits both the conversion of PrP^C to PrP^{Sc} in PMCA [101] and the formation of fibrils of recombinant PrP in the amyloid seeding assay (ASA) [102]. In transgenic mice studies, mice expressing PrP lacking the OR region, and therefore partially lacking copper binding ability, have prolonged incubation times after scrapie inoculation, even when this mutant PrP is overexpressed [105]. However, both insertions [106] and deletions [107] [108] of the copper-binding OR result in human prion disease.

The non-OR copper-binding region has been studied in more detail as of late since it lies next to the HD. The HD, which importantly contains the palindromic motif sequence AGAAAAGA, has recently been suggested to be involved in early structural changes of prion conversion [85]. In fact, studies have found that a change in copper coordination in the non-OR region induces structural changes that extend into this neighboring hydrophobic region. However, studies disagree on whether copper binding to PrP increases or decreases the likelihood of PrP to generate a β-sheet conformation, which is widely interpreted as the first step to PrP^{Sc} formation. One study found that when Cu ions are bound to PrP 90-126 (which exclusively includes the non-OR and HD), the native fold of PrP^C is destabilized and a β-sheet-like transition is observed [86]. Another study on the same region of PrP finds that when copper binds only to the H110 site, β-sheet formation is reduced compared to the apo-peptide [87].

1.3.2.6.1 Disruption of copper binding at PrP H95Y promotes prion conversion

Studies from our lab individually mutated five of the copper binding histidines from the OR and non-OR to tyrosines (a conservative mutation that removes the physiological copper binding ability). By analyzing the conversion susceptibility from PrP^C to PrP^{Sc} *in vitro*, they uncovered that only the mutation in the Non-OR region, H95Y, resulted in a significant increase in prion conversion propensity [73]. When copper is depleted from the medium by CPZ, conversion is increased in WT PrP compared to WT PrP with unaltered copper levels. Interestingly, the conversion propensity of PrP H95Y does not change when copper is chelated, though levels are still elevated compared to WT PrP with or without CPZ addition. This indicates that while copper depletion increases the likelihood for WT PrP to convert into PrP^{Sc}, the same is not true for PrP H95Y. It is possible that the PrP H95Y mutant already converts to PrP^{Sc} at a fast rate and lower copper concentrations have no appreciable effect. Or since the PrP

H95Y mutant already cannot bind copper at the H95Y site, whereas the WT PrP likely loses copper binding at H95 when copper is chelated, this copper binding at H95 is the key interaction for PrP to resist conversion into PrP^{Sc}. In the amyloid seeding assay, they used PTA-isolated PrP^{Sc} seed from ScN2a cells transiently expressing PrP H95Y mutant to seed the conversion of recombinant full-length WT MoPrP. The addition of the H95Y-PrP^{Sc} seed significantly promoted MoPrP fibrillization reactions at both pH 5.5 and 7.0, with shorter lag-phases than the control WT-PrP^{Sc} seed [73].

Using immunofluorescence, they studied the co-localization of PrP H95Y with the 3F4-tag transiently transfected into N2a cells. They found that the PrP H95Y mutant colocalized with organelle markers: EEA1 (early endosomes), Tfn (endosomal recycling compartment), M6PR (late endosome) and LAMP2 (lysosome marker). This suggests that the PrP H95Y mutant predominantly accumulates in the acidic compartments [73]. However, these results would be strengthened using stably transfected cell lines and a colocalization analysis.

1.3.2.6.2 The Non-OR region of the H95Y mutant is less structured in acidic environments than WT PrP

Our lab used X-ray absorption spectroscopy to study the non-OR copper coordination of human PrP^{C} constructs: WT PrP and mutant PrP containing the pathological mutations P102L, Q212P (both indicated in the familial prion disease GSS) and most interestingly for this current work, H95Y. Firstly, they showed that in WT PrP pH modified the non-OR copper coordination. At pH 7 copper is coordinated by H110 alone, but at pH 5.5 copper is anchored to both H95 and H110 in WT PrP [73]. In contrast, in the PrP H95Y mutant (and incidentally, the other two mutants studied as well), pH did not modify the non-OR copper coordination. The mutants have the same copper coordination at pH 7 as WT PrP, but at pH 5.5 they lose the ability to anchor copper at both sites and the metal can only coordinate at H110.

This, along with the *in vitro* work discussed earlier, provides biological and structural evidence that the non-OR region may be critical for prion conversion. It has long been suspected that the unique microenvironments of acidic compartments could act as the cellular site for prion conversion. It was found that WT PrP participates in additional, stabilizing copper coordination in such acidic conditions, while mutants that are unable to participate in the double coordination of copper at H95 and H110 are less stable in such environments and tend to misfold to PrP^{Sc} [73].

Thereby they conclude that when PrP^{C} is only able to coordinate copper with one histidine in the non-OR, it is susceptible to conversion to PrP^{Sc} in acidic conditions,

proposing that the non-OR "may act as the long-sought-after prion switch, critical for disease onset and propagation" [73].

1.3.2.6.3 Spontaneous disease in transgenic mice expressing MoPrP H95Y

Tg mice expressing MoPrP H95Y (Tg H95Y) spontaneously develop prion disease, presenting with neurological symptoms and reduced survival times compared to FVB WT mice (unpublished data Legname Lab). Tg mice highly overexpressing PrP H95Y 6X, have short lifespans when inoculated with scrapie: those with a WT PrP$+/+$ background survived 108 ± 19 days and those on WT PrP$-/-$ background even shorter at 96 ± 6 days.

1.4 Aim of the study

This work seeks to shed light on one of the key events of prion disease, the conversion from PrP^{C} into PrP^{Sc}. The mechanism responsible for this event is still unknown. We have approached this problem by systematically mutating the histidines of the OR and non-OR regions of the N-terminal, hypothesizing that the loss of interaction between copper and histidine may change the conversion propensity of PrP^{C}. One histidine from the non-OR region did cause a change of the prion conversion propensity, H95, and we looked into this residue more closely, performing a amino acid scan at H95, replacing histidine with every other common amino acid. Prion conversion propensity was tested with the prion conversion assay, where exogenous 3F4-tagged PrP containing our mutant of interest was transiently expressed in ScN2a cells, then analyzed by PK digestion for PrP^{Sc} presence.

The resulting amino acid scan revealed a large range of prion conversion propensity depending on the substituted residue. My work was further focused to better understand the results of this preliminary scan, centering on the residues that decreased prion conversion propensity (PrP H95D, H95E, H95K, H95R) and confirming previous work indicating that the residue PrP H95Y increases prion conversion propensity. Our work aims to reproduce the preliminary findings of the amino acid scan, to investigate the involvement of copper chelation on prion conversion with relation to these mutants, to biochemically analyze and to study the localization and trafficking of PrP H95E and PrP H95Y. We anticipate that this work, combined with previous work from our lab, will further our understanding of PrP^{Sc} formation.

Chapter 2

2 Materials and Methods

2.1 Plasmid Construction

2.1.1 Cloning of MoPrP mutants for cell transfection and protein production

The mutations were inserted into pcDNA::MoPrP(1-254)WT, for the generation of stable cell lines, pcDNA::MoPrP(1-254)WT3F4, for transient transfection in ScN2a cells, or pET::MoPrP(23-231), for protein production, with the QuikChange mutagenesis kit (Agilent Technologies) according to manufacturer's instructions. Primers were designed using the Primer Blast (NCBI) and QuikChange Primer Design (Agilent Technologies) (Table 2.1). PCR parameters were as follows: melting temperature: 95°C for 30 sec; annealing temperature: 55°C for 45 sec; extension temperature: 68°C for 5 min. These three steps were cycled 16 times. Strand extension was completed at 72°C for 5 min and reactions cooled to 4°C. 10 ng of template DNA and 2.5 U PfuUltra DNA polymerase was used in each reaction. PCR products were digested by DpnI (1 μL per 20 μL PCR reaction for 1 hour at 37°C) prior to transformation into competent DH5α cells. Bacterial clones containing the plasmid (selected by ampicillin resistance) were cultured O/N. Plasmid DNA was purified using the QIAprep Miniprep Kit (Qiagen). All the constructs were verified by sequencing.

The pET11a expressing the full length MoPrP(23-231) was kindly provided by the group of Prof. Jesus Requena (Universidade de Santiago de Compostela, Spain).

Primer	Sequence
H95D-Forward	CAAGGAGGGGGTACCGACAATCAGTGGAACAAGC
H95D-Reverse	GCTTGTTCCACTGATTGTCGGTACCCCCTCCTTG
H95E-Forward	CAAGGAGGGGGTACCGAGAATCAGTGGAACAAGC
H95E-Reverse	GCTTGTTCCACTGATTCTCGGTACCCCCTCCTTG
H95K-Forward	CAAGGAGGGGGTACCAAGAATCAGTGGAACAAGC
H95K-Reverse	GCTTGTTCCACTGATTCTTGGTACCCCCTCCTTG
H95R-Forward	CAAGGAGGGGGTACCAGGAATCAGTGGAACAAGC
H95R-Reverse	GCTTGTTCCACTGATTCCTGGTACCCCCTCCTTG
H95Y-Forward	CAAGGAGGGGGTACCTATAATCAGTGGAACAAGC
H95Y-Reverse	GCTTGTTCCACTGATTATAGGTACCCCCTCCTTG

Table 2.1: Primers used for MoPrP mutagenesis at H95

2.1.2 Cloning of full-length MoPrP H95E plasmid for Tg mice construction

The pJB1:: MoPrP(1-254)H95E was amplified from pcDNA::MoPrP(1-254)H95E by PCR using these primers:

- 5'Bsi-MoPrP: 5'-CCT AGT GGT ACC TCG TAC GCA GTC ATC ATG GCG AAC CTT GGC TAC TGG-3'

- 3'Fse-MoPrP: 5'-CGC TCA CAA TCG CGG CCG GCC TCA TCC CAC GAT CAG GAA GAT GAG G-3'

The PCR products were then ligated into pJB1 (modified vector from MoPrP.Xho vector [5], in which BsiWI and FseI sites replaced the XhoI site) using the BsiWI and FseI restriction sites. The PCR were performed using the Phusion DNA polymerase (New England Biolab) according to manufacturer's instructions. Plasmid DNA was purified using the QIAprep Miniprep Kit (Qiagen). All the constructs were verified by sequencing.

The pJB1 was kindly provided by the group of Prof. Glenn Telling (Colorado State University, USA).

2.2 Cell Cultures

2.2.1 Cell lines

- N2a mouse neuroblastoma cells were purchased from the American Type Tissue Collection (ATCC CCL131).
- N2aPrP$-/-$ cells [6] were kindly provided by the group of Dr. Gerold Schmitt-Ulms (University of Toronto, Canada).
- ScN2a cells are N2a cells chronically infected with the Rocky Mountain Laboratory (RML) prion strain.

2.2.2 Cell growth

N2a, N2aPrP$-/-$ and ScN2a cells were cultured in minimal essential medium with Earle's salts (EMEM, Invitrogen) supplemented with 10% heat-inactivated fetal calf serum, 1% nonessential amino acids and 1% penicillin-streptomycin in a humidified atmosphere of 5% CO_2 at 37°C. Complete medium was changed 2-3 times weekly. All cell culture work was carried out with strict aseptic technique. When cells reached 80-90% confluence they were harvested, sub-cultured or cryopreserved.

2.2.3 Cell harvesting

Cells were harvested from 10 cm cell plates in 400 μL cold lysis buffer (10 mM Tris HCl pH 8.0, 150 mM NaCl, 0.5% Nonidet P-40 substitute, 0.5% sodium deoxycholate). Cell debris was removed by centrifugation at 2600 rpm for 10 min at 4°C in a bench microcentrifuge (Eppendorf). An aliquot was taken for total protein quantification by bicinchoninic acid (BCA) assay kit (Pierce) and the remaining supernatant was stored at -20°C until use.

2.2.4 Cell transfection

Cell transfections were performed using Effectene transfection reagent (Qiagen) following the manufacturer's guidelines. For transient transfections cell lysates were collected 72 hours post-transfection for further analysis. For stable transfections, 24 hours after transfection, cells were cultured in the selective medium, comprised of complete medium additionally supplemented with 0.3 mg/mL Geneticin (Invitrogen) (optimal Geneticin concentration for this cell line, N2aPrP$-/-$, was determined by a dose response curve).

The selective medium was changed every 3-4 days for about five days when most Geneticin-sensitive cells had died. After that, individual cells were isolated in 96-well plates by limiting dilution. Clones were expanded from individual cells, harvested for Western Blot analysis of PrP expression levels and cryopreserved for subsequent use. Stably transfected cell lines were maintained in complete medium supplemented with 0.3 mg/mL Geneticin (unless specified otherwise).

2.2.5 Cuprizone (CPZ) treatment

ScN2a cells were transiently transfected with mutant MoPrP (see Section 2.2.4). After 24 hours the medium was replaced with complete medium supplemented with 10μM CPZ in 50% ethanol. Controls were cultured with an equal amount of 50% ethanol. Cell lysates were collected after 48 hours of CPZ treatment.

2.2.6 Cell viability

To check cell viability of ScN2a cells transiently transfected with plasmids, cells were seeded in a 96-well tissue culture plate one day before transfection and then transiently transfected with MoPrP constructs. Seventy-two hours after the transfection the MTT assay was performed. To check the viability of stably transfected cell lines, cells were seeded in a 96-well tissue culture plate, cultured for 48 hours and the MTT assay was carried out.

The MTT assay was performed as follows: the medium was removed and the cells were incubated with 200 μL of MTT (Sigma) working solution (5 mg/mL of MTT in sterile PBS 1X) for 4 h at 37°C. Cell viability was assessed by the conversion of MTT (yellow) to a formazan product (purple). The solution was removed and formazan products were dissolved by adding 200 μL of DMSO to each well. The optical density was read at 570 nm and the background subtracted at 690 nm using a VersaMax plate reader (Molecular Device). Each assay was performed in duplication of 5 wells.

2.3 Protein Detection

2.3.1 SDS-polyacrylamide gel electrophoresis (SDS-PAGE)

Protein loading buffer 2X (LB; 10% glycerol, 50 mM Tris HCl pH 6.8, 2% SDS, 4M Urea, bromophenol blue and 0.2M DTT added fresh) was added to samples containing a determined amount of total protein, ascertained by BCA. Samples were then boiled at

100°C for 5 min. Then samples were spun down before loading onto 12% Tris-Glycine gels. Gels were electrophoresed for 150 min at 100 V (or until the dye front ran off the end of the gel). PageRuler Prestained Protein Ladder (Thermo Scientific) was used as a molecular weight marker.

2.3.2 Coomassie staining of gels

After electrophoresis, to visualize proteins directly on the gel, gels were stained in Coomassie ProBlue Safe Stain (Giotto Biotech) according to manufacturer's directions, repeating the final rinse until the protein bands were clearly visible.

2.3.3 Western blot

After electrophoresis, protein was transferred onto Immobilon PVDF membranes (Millipore) at 250 mA for 180 min or 30V overnight by wet transfer in Criterion Blotter (Bio-Rad). A Ponceau S Staining Solution (0.1%(w/v) Ponceau S in 5%(v/v) acetic acid) was applied to membranes to ensure efficiency of transfer, then rinsed away completely with distilled water. Membranes were then blocked with 5% nonfat milk powder in TBS-T (0.05% Tween), incubated with 1:1000 anti-PrP 3F4 antibody (epitope: human specific M109-M112) and/or 1:1500 anti-PrP W226 antibody (epitope: W144-N152), then incubated with the HRP-conjugated secondary antibody Goat anti-Mouse at 1:1000 and developed by enhanced chemiluminescence (ECL, GE Healthcare). As a load control anti-βActin conjugated with HRP was also assessed after HRP-inactivation of the membranes. Band intensity was acquired using the UVI Soft software (UVITEC, Cambridge). Finally, band intensities were quantified relatively using ImageJ by densitometric analysis [135].

2.4 Biochemical Assays on PrPSc and PrP^C

2.4.1 Proteinase-K (PK) digestion

The accumulation of PK-resistant PrP in cell lysates was detected by proteinase K (PK) digestion followed by immunoblotting. For each sample, 500 μg of total protein, 20 μg/mL PK (Roche, ratio protein:PK = 50:1) and lysis buffer added to a final volume of 0.5 mL was prepared. Samples were then incubated at 37°C for one hour. The reaction was stopped by adding PMSF at a 2 mM final concentration. PK digested products were precipitated by centrifugation at 100,000 x g for 1 hour at 4°C in an

ultracentrifuge (Beckman Coulter) and resuspended in LB 2X. All samples were boiled for 10min at 100°C, then stored at -20°C until analysis by immunoblotting.

2.4.2 Protein deglycosylation by Endo H or PNGase F

For the glycosidase assays, 30 μg total protein of cell lysates were treated with Endo H or PNGase F enzymes (New England Biolabs), following manufacturer's instructions. Briefly, 1 μL of 10X glycoprotein denaturing buffer (provided with the kit) was added to the cell lysates and the samples were boiled for 10 minutes at 100°C. Samples were chilled on ice and spun down. Next, for Endo H digestion, 2 μL 10X Glyco Buffer 3 and 1 μL of Endo H were mixed into the reaction; while for PNGase F digestion 2 μL Glyco Buffer 2 (10X), 2 μL 10% NP-40 and 1 μL of PNGase F were mixed in. Samples were incubated overnight at 37°C. Finally, LB 2X was added and samples were boiled for 10 min at 100°C to stop the reaction, then stored at -20°C until analysis by immunoblotting.

2.4.3 Solubility Assay

Cell lysates containing 100 μg of total protein was adjusted to a final volume of 500 μL in lysis buffer containing PMSF (final concentration 2 mM). Samples were incubated on ice for 20 min before centrifugation at 100,000 x g for 1 hour at 4°C in an ultracentrifuge (Beckman Coulter). The supernatant was recovered, collected by acetone precipitation and resuspended in 50 μL TGS buffer for further analysis by immunoblot. The pellet was washed twice by resuspension in 500 μL lysis buffer containing PMSF and recovered by centrifugation at 100,000 x g for 1 hour at 4°C in an ultracentrifuge (Beckman Coulter). The pellet was resuspended in 50 μL TGS buffer for further analysis by immunoblot.

2.5 Immunofluorescence

2.5.1 Immunofluorescence for the detection of PrP and organelles

Cells were cultured on poly-L-lysine coated coverslips for 24 h. Medium was removed and cells were fixed with 4% paraformaldehyde (PFA) in phosphate-buffered saline (PBS) for 20 min at RT. Cells were washed 3X for 5 min with PBS then permeabilized with 0.3% Triton X-100 in PBS for 10 min and subsequently blocked in 7% NGS in

PBST (PBS 1X + 0.05% Triton X-100) for 1 hr at RT. After blocking, cells were incubated in the primary antibody in 1% NGS in PBST in a humidified chamber O/N at 4°C. The next day coverslips were washed 4X with PBS 1X, incubated with the secondary antibody conjugated with Alexa Fluor in 1% NGS in PBST for 1 hr at RT in the dark, and washed 2X in PBS 1X. Finally, cells were incubated in DAPI (1:500) in PBST for 15 min and washed a final time with PBS 1X. Coverslips were air dried and mounted on coverslips using Vectashield (VECTOR Laboratories), allowed to dry, sealed and stored in the dark at 4°C.

2.5.2 Immunofluorescence for the surface staining of PrP

Cells were cultured on poly-L-lysine coated coverslips for 24 h. Cells were then placed on ice for 20 min, after the medium was replaced with medium containing the primary antibody for 30 min washed 1X in PBS 1X still on ice. Cells were fixed with 4% paraformaldehyde (PFA) in PBS for 20 min at RT. Cells were washed 3X for 5 min with PBS 1X then incubated with the secondary antibody conjugated with Alexa Fluor in 1% NGS in PBS 1X for 1 hr at RT in the dark, and washed 2X in PBS 1X. Finally, cells were incubated in DAPI (1:500) in PBST for 15 min and washed a final time with PBS 1X. Coverslips were air dried and mounted on coverslips using Vectashield (VECTOR Laboratories), allowed to dry, sealed and stored in the dark at 4°C.

2.5.3 Antibodies used for immunofluorescence

The primary antibody used to detect PrP was W226 at 1:200. The organelle markers primary antibodies, purchased from Abcam, were the ER marker (anti-Calnexin), the early endosome marker (anti-EEA1), the recycling endosome (anti-Transferrin receptor Tfn), the late endosome marker (anti-Mannose-6 phosphate receptor M6PR) and the lysosome marker (anti-LAMP1), all used at 1:400. Secondary antibodies (used at 1:400) were Alexa Fluor-488 goat anti-mouse for W226 and Alexa Fluor-594 goat anti-rabbit for the organelle markers.

2.5.4 Image Acquisition

Images were acquired with a Nikon Eclipse Ti confocal microscope equipped with NIS Elements Nikon Confocal Software.

2.6 Preparation of scrapie cell seed by sodium phosphotungstic acid (PTA)

1 mg of ScN2a or N2aPrP$-/-$ cell lysate was used for PTA precipitation by adding 500 μL of PBS 1X containing 4% sarkosyl, PMSF (final concentration 2 mM) and 0.5% PTA, with constant shaking 300 rpm, at 37°C for 1 hour and centrifuged 14,000 g for 30 min at RT. The pellet was washed with 500 μL of PBS 1X containing 2% Sarkosyl and PMSF (final concentration 2 mM) then centrifuged again at 14,000 g for 30 min at RT. The pellet was washed a final time with 500 μL of PBS 1X and centrifuged a final time at 14,000 g for 45 min at RT. After that, the supernatant was discarded and the pellet was resuspended in 150 μL of PBS 1X and stored at -20°C until use.

2.7 Preparation of recombinant proteins

2.7.1 Protein expression

Recombinant MoPrP(23-231) and MoPrP-H95E(23-231) were expressed and produced in E. coli Rosetta DE3 bacteria grown in LB medium (10g tryptone, 5 g yeast extract, 10 g NaCl) as follows. Freshly transformed 100 mL overnight culture of Rosetta DE3 bacteria divided equally among 3 flasks of 750 mL each of LB medium plus ampicillin (100 μg/mL). These were grown at 37°C with vigorous shaking until the OD600 reached 0.5 at which point they were induced with IPTG (at 0.8mM), and grown O/N at 37°C with vigorous shaking. Cells were harvested by centrifugation at 4000 g, 4°C for 30 min.

2.7.2 Isolation of inclusion bodies

The bacteria pellet was resuspended in 25 mM Tris-HCl, 5 mM EDTA, 0.8% Triton X-100, 0.4% Deoxycholic acid, 1 mM PMSF, pH 8 and lysed by Panda Plus homogenizer at 4°C. Bacteria cells were disrupted by three cycles of mechanical lysis at 1500 bar. Inclusion bodies (IBs) were collect by centrifugation at 10,000 g, 30 min, 4°C, washed once with washing buffer (25 mM Tris-HCl, 5 mM EDTA, 0.8 % Triton X-100, pH 8), and then again with cold water twice. Washed IBs were solubilized in 5 volumes of 8 M GdnHCl, and then bacterial debris was removed by centrifugation at 10,000 g, 30 min, 4°C.

2.7.3 Protein purification

The dissolved IBs in 8 M GdnHCl were diluted to 6 M GdnHCl using 50 mM Tris, 1 M NaCl, pH 8.0 then loaded onto a 5mL HisTrap crude column (GE Healthcare) in binding buffer (2 M GdnHCl, 500 mM NaCl, 20 mM Tris, 20 mM imidazole, pH 8.0). After that, the column was washed with 3 column volumes of binding buffer and eluted with a gradient from 0-100% of elution buffer (5 M GdnHCl, 500 mM NaCl, 20 mM Tris, 500 mM imidazole, pH 8.0) at 5 mL/min in 20 min. Finally, the PrP-contained fractions were loaded onto the gel filtration column (Superdex 200 26/60, GE) and eluted with 6 M GdnHCl, 25 mM Tris-HCl, 5 mM EDTA, pH 8 at a flow rate of 2 mL/min. Purified protein was analyzed by SDS- PAGE and Coomassie staining. Protein concentration was determined by UV at 280 nm and stored at -20°C until use.

2.7.4 Protein refolding

Purified prion proteins were rapidly diluted to a final concentration of 0.1 mg/mL using 25 mM Tris, 5 mM EDTA, pH 8.0. Then the samples were dialyzed against refolding buffer (20 mM NaOAc, 0.005% NaN3, pH 5.5) using a 3 kDa molecular weight cut-off (MWCO) membrane (Spectra/Por), until a final GdnHCl concentration of about 10 μM.

2.8 Generation and detection of transgenic mice

MoPrP mutant transgenes (H95E) containing mouse regulatory sequences were excised from the plasmid pJB::MoPrP(1-254, H95E) with the restriction endonuclease NotI. These fragments were microinjected into the pronucleus of 200 fertilized FVB mice eggs, which were implanted into pseudopregnant FVB females. This work was done at the transgenic mouse facility of Cyagen Biosciences Inc (USA).

DNA collected from the tails of F0 offspring mice was used to screen for transgene integration by a PCR assay using specific primers. The primers used were 5'-GAA CTG AAC CAT TTC AAC CGA G-3' and 5'-AGA GCT ACA GGT GGA TAA CC-3'. The presence of PCR-amplified products of 800 bp indicated the presence of MoPrP mutant transgenes. Transgenic F0 mice were crossed with WT mice to obtain an F1 generation that was also screened using PCR amplification as above. Unfortunately, no F1 offspring containing the transgene were obtained. This work with transgenic mice was performed in collaboration with the group of Prof. Juan-Maria Torres at Centro de Investigacion en Sanidad Animal (CISA-INIA), Madrid, Spain.

2.9 Statistical analysis

Western blot protein bands were relatively quantified by densitometry with ImageJ. When possible (i.e. samples analyzed without PK digestion), PrP bands were normalized to β-actin as an internal control of load control (total protein was also quantified by BCA and equal amounts added to each well). Then PrP variable were analyzed as a ratio of WT PrP levels. For experiments with transfection, an additional level of calculation was necessary to account for the transfection efficiency of each sample. To this aim we calculated the ratio of the PK digested protein band of the sample with the anti-PrP 3F4 antibody with respect to the PK digested protein band PrP WT with anti-PrP 3F4, then compared this to the ratio of the non-PK digested protein band of the sample normalized to β-actin with respect to the non-PK digested PrP WT 3F4 within each gel.

For the experiments with CPZ, a similar approach was used, but we included an equal external loading control in each gel as a reference to compare WT PrP levels between gels to quantify the variance of WT PrP samples to avoid variance heterogeneity.

When applicable we used a one-way analysis of variance (one-way ANOVA), if differences among means were found to be statistically significant, we performed the post hoc multiple comparisons test with the mean of the WT group, using the Dunnett's multiple comparison to account for the family-wise error rate when performing multiple comparisons. Each p-value is adjusted to account for multiple comparisons, with family-wise significance, at 0.05.

Chapter 3
3 Results

3.1 Amino acid scanning of H95 reveals a "hot spot" for prion conversion

In previous work in our lab, five of the copper binding histidines from the OR and non-OR regions were individually mutated to tyrosine, a conservative mutation that removes the physiological copper binding ability. By analyzing the conversion susceptibility from PrP^{C} to PrP^{Sc} *in vitro*, they uncovered that only the mutation in the non-OR region, H95Y, resulted in a significant increase in prion conversion propensity [73].

Intrigued with the H95 site, we wondered if other amino acid substitutions would have similar effects on prion conversion. To this effect, we completed an amino acid scan of H95, replacing the histidine with every other common amino acid and measuring the prion conversion propensity. This was done with the prion conversion assay, a method to quantify the conversion of PrP^{C} to PrP^{Sc}. We transiently expressed our mutant PrPs of interest into N2a cells chronically infected with RML prions (ScN2a). Fundamental to this method, exogenous PrP that is transiently transfected into ScN2a cells can convert into PrP^{Sc}. We transiently transfected ScN2a cells with our PrP mutants of interest, collected the cell lysates 72 hours later and analyzed by PK digestion and immunoblot. To discriminate between endogenous and exogenous PrP, the 3F4 tag, a human-specific epitope with methionine substitutions at residues 108 and 111, was added to all constructs and later detected by the 3F4 antibody [30] [1] [2] [3]. The 3F4 antibody was confirmed to be specific for 3F4-tagged PrP (Figure 3.1**A**). We also confirmed that this tag does not influence endogenous protein expression or prion conversion (Figure 3.1**B**).

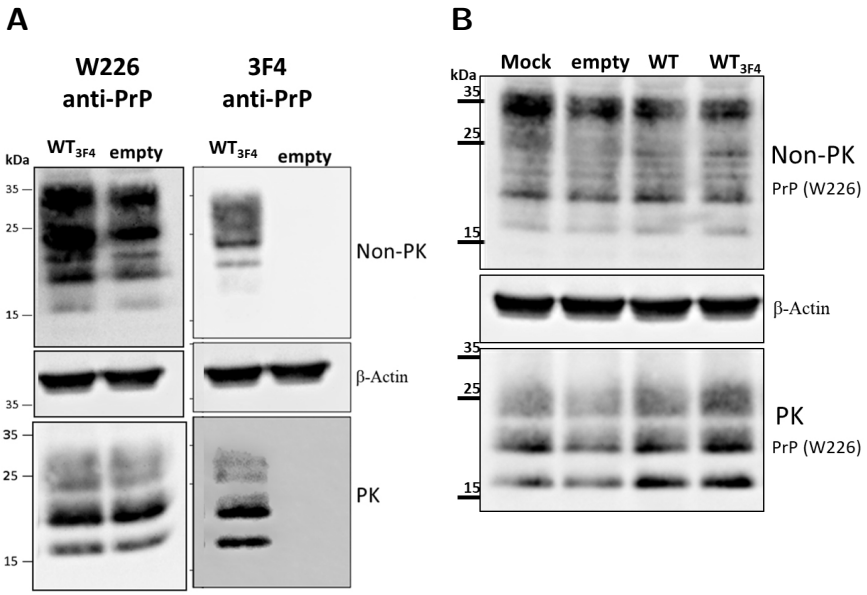

Figure 3.1: Anti-PrP 3F4 antibody is specific to the 3F4 epitope tag and does not disrupt prion conversion. (**A**) PK digested and non-PK digested samples were blotted first with anti-PrP 3F4, then stripped and blotted with anti-PrP W226 Antibody. We detect no cross-reactivity with native mouse PrP, seen here in the cells transfected with the empty vector, and specific recognition of PrP containing the 3F4 epitope, as seen in lanes with PrP WT_{3F4}. (**B**) Western blot comparison of ScN2a cells without transient transfection (Mock), expressing an empty vector (empty), expressing the MoPrP construct (WT), or the MoPrP construct with the 3F4-tag (WT_{3F4}). No effect of 3F4-epitope tag on PrP expression and PK-resistance was detected.

Western blot analysis of total PrP expression level (endogenous and exogenous) by the W226 antibody revealed no differences either before or after PK digestion. The expression level of exogenous PrP, as detected by the 3F4 antibody, showed similar PrP expression levels among all constructs without PK digestion Figure 3.2 (A). Importantly, after PK digestion, there are marked changes in the prion conversion propensity of the constructs Figure 3.2. When H95 was substituted with a neutral or small amino acids (A, G, C, S, T, N, Q, P), the PrP^{Sc} levels were comparable to WT. However, when H95 was replaced by hydrophobic amino acids (F, Y, L, M, V, W, I), the PrP^{Sc} levels were dramatically increased. The cases of V, F, Y, and I had the highest increase of prion conversion, with levels 2-3 times higher than WT. On the other extreme, substitutions with the charged amino acid residues (D, E, K, R) had a low rate of PrP^{Sc} conversion, suggesting that these substitutions somehow dissuade prion conversion.

These data suggest that the fifth copper binding site, H95, is a "hot spot" for prion conversion since by amino acid substitutions at this position, the prion conversion

propensity is highly promoted or inhibited, possibly dependent on the hydrophobicity of the substituting amino acid.

This amino acid scan was a preliminary screening with a sample size of 2. It has the potential to be highly interesting, and as such, requires much study. In this work we have focused on the charged side chains that decrease the conversion propensity, doing extensive studies to confirm this preliminary result and shed some light on the mechanisms involved behind these stunning findings.

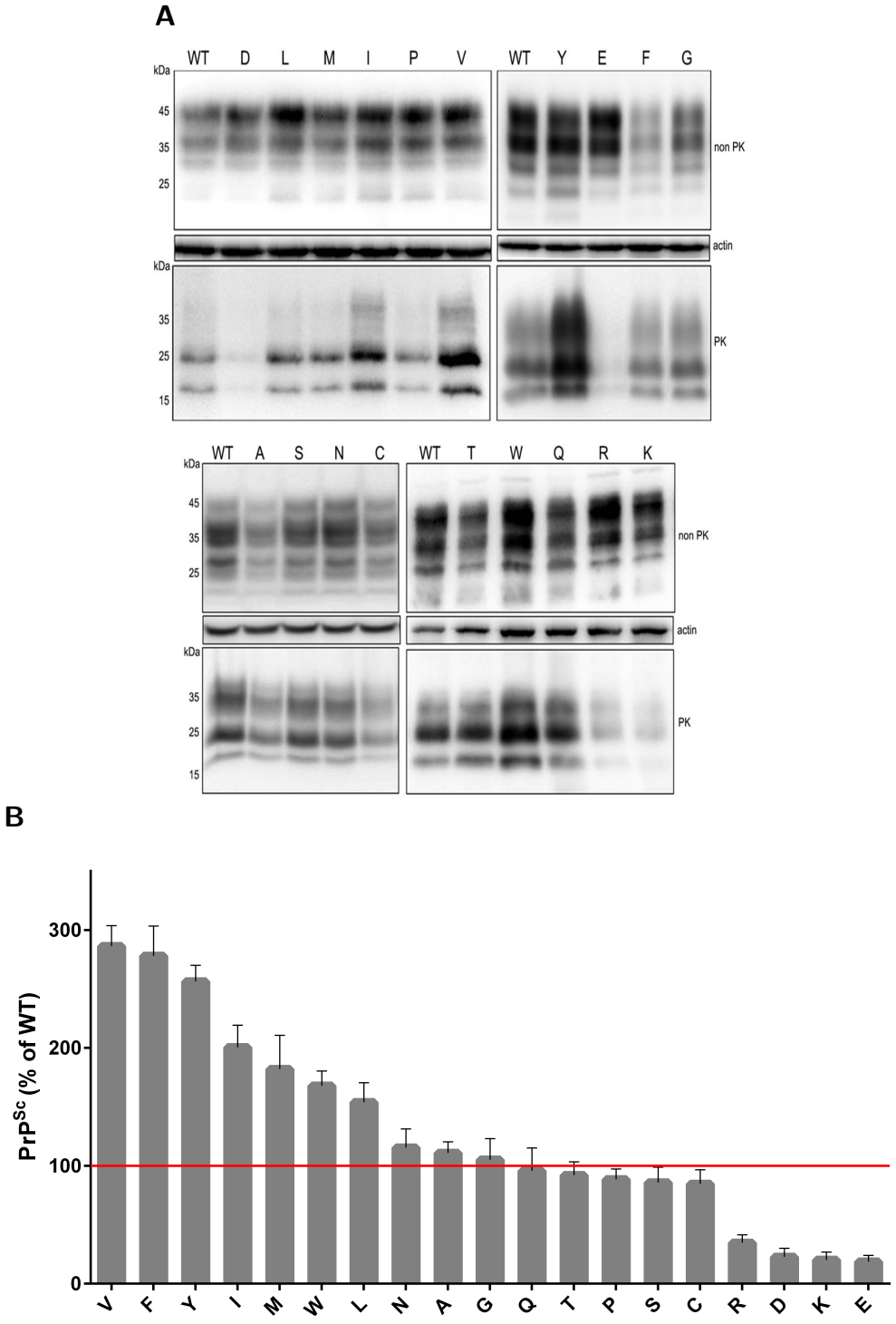

Figure 3.2: Effect of amino acid substitutions at H95 on prion conversion (**A**) Fifty μg of undigested cell lysates from ScN2a cells expressing 3F4-tagged WT and mutant PrPs were applied to each lane. Five hundred μg of cell lysates were digested with PK at 37°C for 1 hour. Exogenous 3F4-tagged PrP was detected by the anti-PrP 3F4 antibody. B-actin was used as an internal loading control. (**B**) Quantitative analysis of PK-resistance levels (PrP^{Sc}) in transfected constructs.

3.2 H95 substituted with amino acids containing charged side chains reduces prion conversion *in vitro*

To confirm the preliminary results of the amino acid scan in the mutants which decreased prion conversion propensity, we again utilized the prion conversion assay.

The following constructs were used: MoPrP WT_{3F4}, MoPrP $H95D_{3F4}$, MoPrP $H95E_{3F4}$, MoPrP $H95K_{3F4}$, MoPrP $H95R_{3F4}$ (and additionally MoPrP $H95Y_{3F4}$ as another control of the experiment to compare with previous results) and an empty vector lacking PrP and the 3F4 tag (hereby referred to as WT_{3F4}, $H95D_{3F4}$, $H95E_{3F4}$, $H95K_{3F4}$, $H95R_{3F4}$, $H95Y_{3F4}$ and empty, respectively). ScN2a cell viability was not affected by transient transfection of any of the constructs, indicating that the expression of PrP WT_{3F4} and mutants had no toxic effect on ScN2a cells (Figure 3.3).

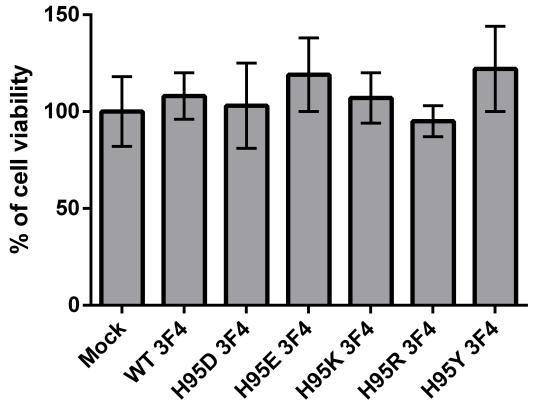

Figure 3.3: Mutant constructs transiently transfected into ScN2a cells do not decrease cell viability, as tested with MTT assay. Quantitative analysis of the cell viability percentage in transfected constructs relative to mock transfected ScN2a cells (n=3).

Analysis of the total PrP expression level (endogenous and exogenous) by the W226 antibody revealed no differences either before or after PK digestion, so transfection with mutant PrP did not alter ScN2a cells' ability to express PrP (Figure 3.4). Analysis of exogenous PrP by the 3F4 antibody showed similar exogenous PrP expression level among all constructs without PK digestion, as determined by one-way ANOVA ($F(5,24)=1.308$, $p=0.2936$). Therefore, expression of the exogenous protein in the cell was not affected by the mutant type (Figure 3.5**A**, 3.5**B**).

Importantly, after PK digestion, we were able to confirm the marked changes in the prion conversion propensity of the constructs. In line with our preliminary, exploratory experiment, compared to WT_{3F4} PrP^{Sc}, the mutants $H95D_{3F4}$ (M=26.96%, SD=19.02%), $H95E_{3F4}$ (M=27.48%, SD=23.11%), $H95K_{3F4}$ (M=34.74%, SD=10.70%), and $H95R_{3F4}$ (M=65.19%, SD=22.42%) had reduced PrP^{Sc} and $H95Y_{3F4}$ (M=348.5%, SD=132.2%) increased PrP^{Sc} (Figure 3.5**A**, 3.5**C**). With this we contribute the first robust evidence of these mutations' ability to decrease prion conversion propensity.

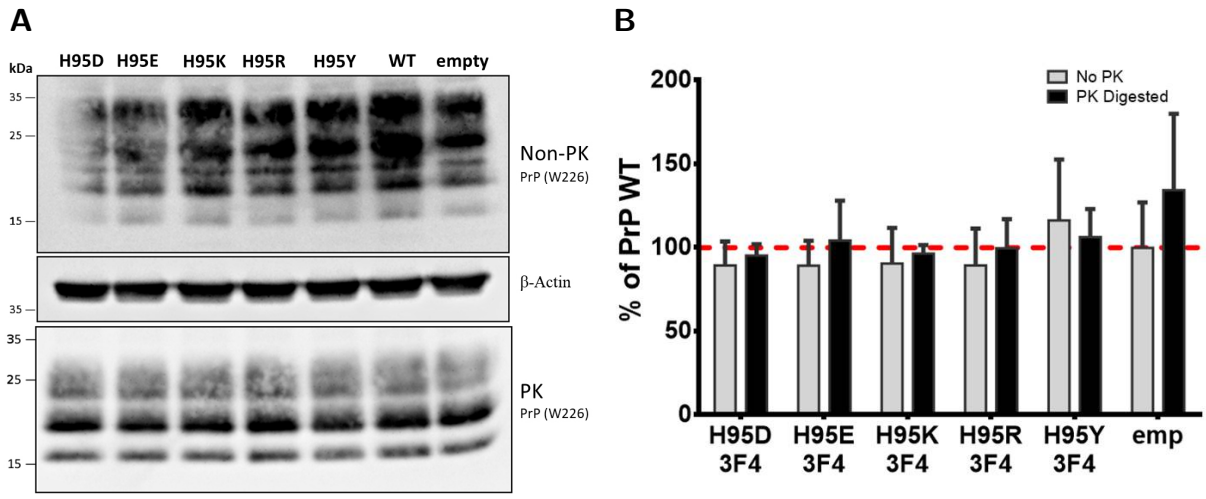

Figure 3.4: Total PrP expression level was similar in all ScN2a cells transiently transfected with 3F4-tagged mutant PrPs for prion conversion assay experiments. (**A**) PrP detected by anti-PrP W226 antibody without and with PK digestion. β-actin was used as an internal loading control. (**B**) Quantitative analysis of β-actin-normalized total PrP expression levels without and with PK digestion (n=5).

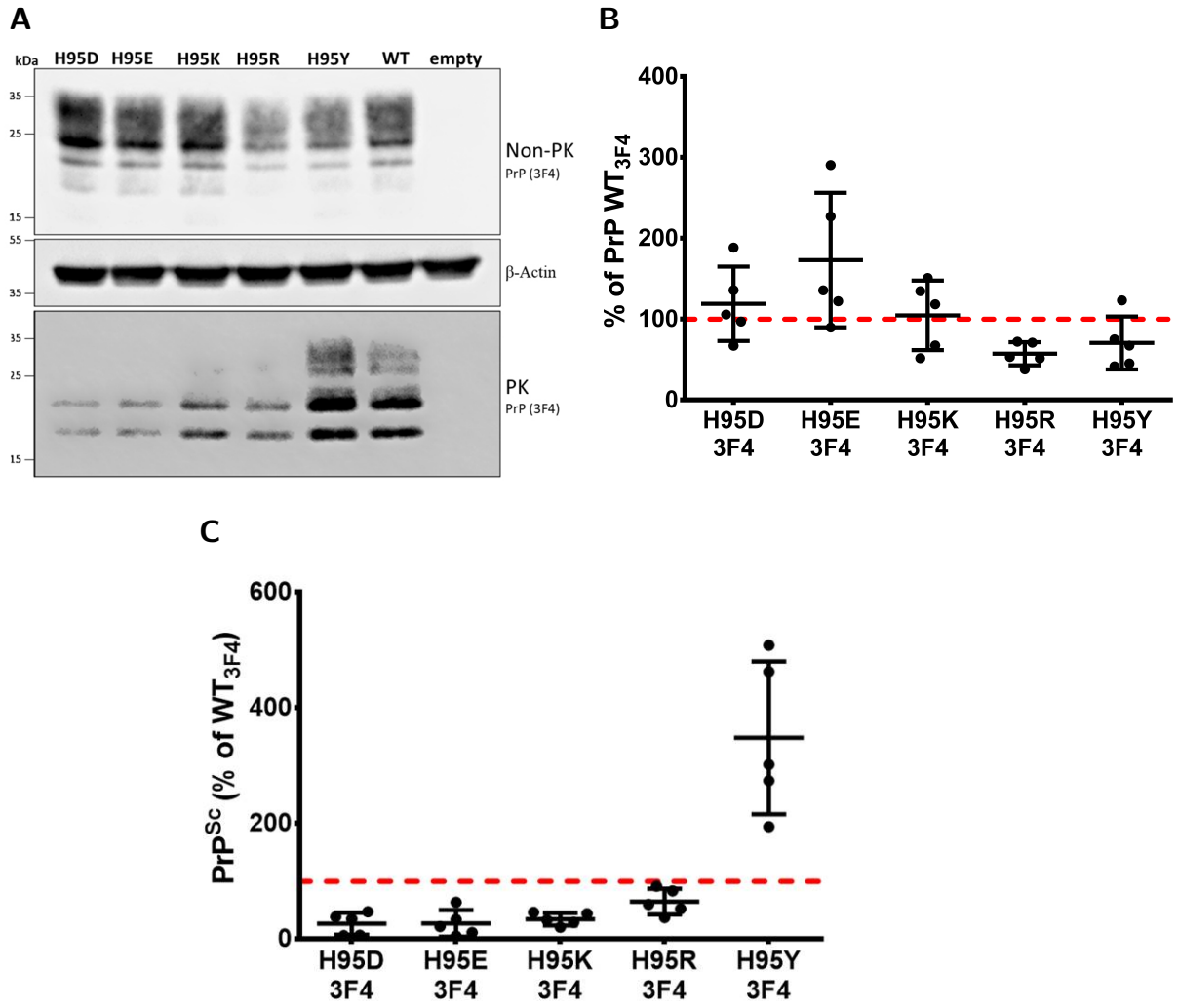

Figure 3.5: The H95 substitution with charged amino acids impedes prion conversion and confirmation of H95Y increasing prion conversion. (**A**) Forty μg of undigested cell lysates from ScN2a cells expressing 3F4-tagged WT and mutant PrPs were applied to each lane. Five hundred μg of cell lysates were digested with PK at 37°C for 1 hour. Exogenous 3F4-tagged PrP was detected by the anti-PrP 3F4 antibody. B-actin was used as an internal loading control. (**B**) Quantitative analysis of non-PK digested expression levels of exogenous mutant PrP compared to PrP WT_{3F4}. (**C**) Quantitative analysis of PrP^{Sc} PK-resistance levels in transfected constructs. PK resistant mutant PrP is represented in the graph as a percent of PK digested PrP WT_{3F4}, with transfection efficiency (n=5).

For further studies we chose to focus the PrP mutation with the lowest prion conversion propensity: H95E. Additionally, we used PrP WT as a control and continued to analyze PrP H95Y as a positive control, consistently comparing these to appreciate any small differences by comparing the WT and the two extremes of prion conversion.

3.3 Chelation of copper slightly increased prion conversion propensity in PrP H95E and WT PrP

WT PrP can coordinate up to six copper ions in the N-terminal, but the mutation at H95 removes one of these copper binding sites. We investigated the effect general depletion of copper would have on our system. To explore this we used the prion conversion assay, described in Section 3.1, where we treated ScN2a cells transiently transfected with WT_{3F4}, $H95D_{3F4}$, $H95E_{3F4}$, $H95K_{3F4}$ or $H95R_{3F4}$ and treated the cells with 10 μm of the copper chelator cuprizone (CPZ). After 48 of hours CPZ treatment, PK-resistance levels were evaluated.

The CPZ treatments had no significant effects on the prion conversion propensity of any of the transfected PrPs compared to the same transfected PrP without CPZ (Figure 3.6). We see again the basic trends noticed before, but the removal of copper from the medium while not statistically significant, did show a trend of moderately increasing prion conversion, especially in PrP H95E CPZ, with a 37.05% increase compared to PrP H95E and PrP WT CPZ, with a 38.74% increase compared to PrP WT.

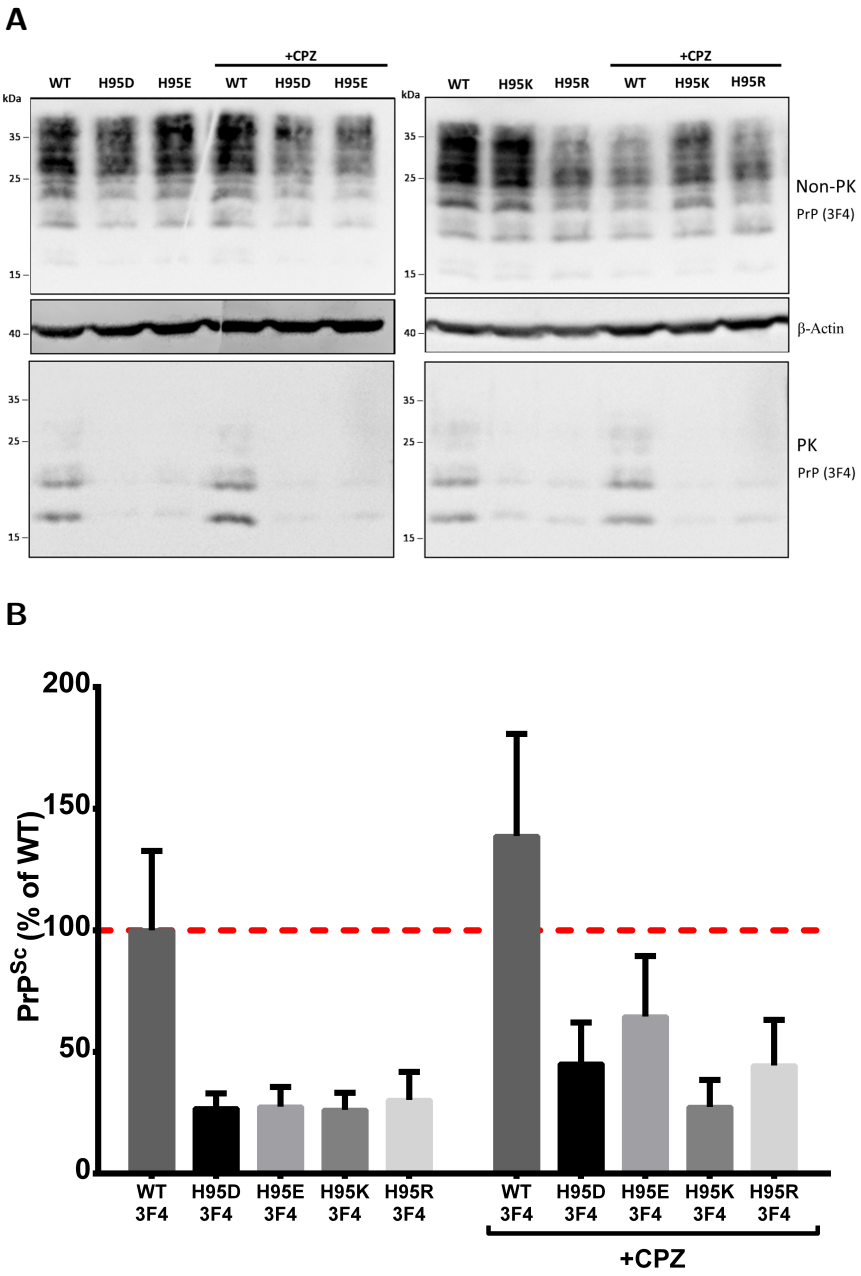

Figure 3.6: Copper chelation moderately raised prion conversion propensity in PrP H95E and WT PrP. (**A**) After transfection, ScN2a cells were treated with 10 μm CPZ for 48 hours. Forty μg of undigested cell lysates from ScN2a cells expressing 3F4-tagged WT and mutant PrPs with or without CPZ treatment were applied to each lane. Five hundred μg of cell lysates were digested with PK at 37°C for 1 hour. Exogenous 3F4-tagged PrP was detected by the anti-PrP 3F4 antibody. B-actin was used as an internal loading control. (**B**) Quantitative analysis of PrP^{Sc} PK-resistance levels in transfected constructs with or without CPZ treatment PK resistant mutant PrP is represented in the graph as a percent of PK digested WT PrP, with transfection efficiency (n=4).

3.4 Biochemical features of PrP H95E

3.4.1 Generation of stable cell lines expressing PrP WT and H95 mutants from N2aPrP$-/-$ cells.

To study the biochemical features of the H95E mutant, we created Geneticin-resistant monoclonal stable cell lines from N2aPrP$-/-$ cells: N2aPrP$-/-$ WT, N2aPrP$-/-$ H95E, N2aPrP$-/-$ H95Y. These cell lines do not contain the 3F4 tag and express only PrP WT, with PrP reintroduced; or express PrP H95E or PrP H95Y, each of which only differ from PrP WT by this single amino acid. The expression of the mutant PrP was not toxic to the cells, indicating that genomic expression of WT PrP, PrP H95E or PrP H95Y do not have a toxic effect on N2a$-/-$ cells (Figure 3.7**B**). One clone of each condition which expressed PrP at levels closest to those found in N2a cells was selected for further experiments (Figure 3.7**A**).

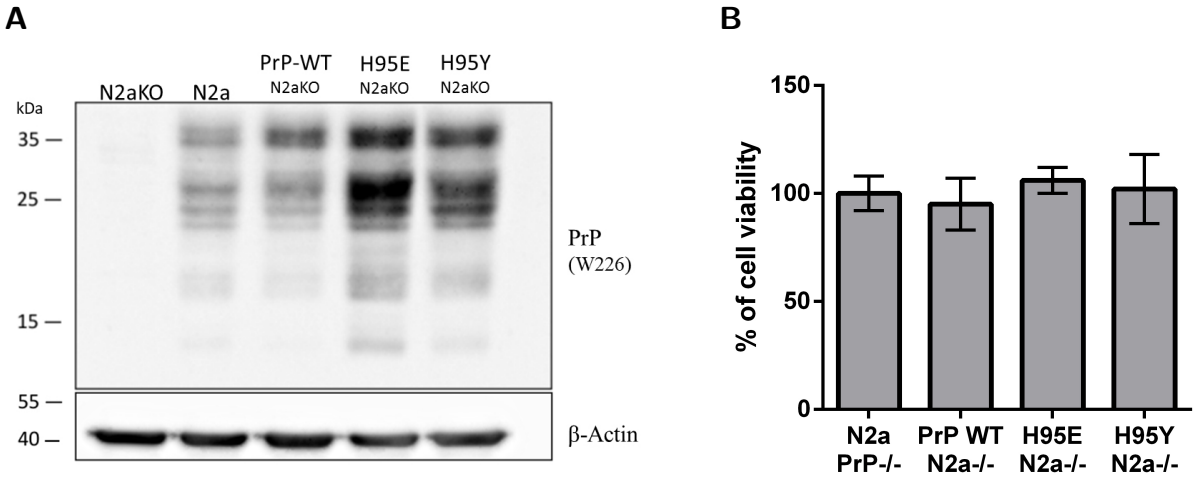

Figure 3.7: Expression of PrP in N2aPrP$-/-$ cells. (**A**) Forty μg of cell lysates were loaded into each lane and PrP was detected with anti-PrP W226 antibody. β-actin was used as an internal loading control. (**B**) MTT assay of stably transfected cell lines: N2a PrP$-/-$ H95E, N2a PrP$-/-$ H95Y, N2a PrP$-/-$ WT, showed no decrease in cell viability compared to N2a$-/-$ cells (n=3).

3.4.2 PrP H95E shares similar glycosylation patterns with PrP WT

To further determine if the prion conversion propensity differences observed could be explained by altered maturation processes, we studied the innate glycosylation patterns and those resulting from glycosidase digestion. Western blot analysis showed that PrP H95E, PrP H95Y and PrP WT all share the same glycosylation patterns, migrating with the classical three bands composed of the diglycosylated, monoglycosylated and unglycosylated PrP (Figure 3.8**B**, untreated lanes).

Next, to monitor proper processing of the posttranslational addition of N-linked oligosaccharide chains and PrP translocation from the ER to the Golgi (explained in detail in Section 1.2.2) of PrP H95E, PrP H95Y and PrP WT, we treated cell lysates to Endo H or PNGase F digestion. Endo H sensitivity is a sign of an immature protein that has not been properly processed through the Golgi [4]. PNGase F will cleave all N-linked oligosaccharide chains from PrP. We found that all of our cases (PrP H95E, PrP H95Y and PrP WT) were resistant to Endo H digestion and showed no differences between them (Figure 3.8**A**). Also, treatment with PNGase F in all cases resulted in two bands, the unglycosylated full length PrP (fl) and the C1 fragment of PrP (C1) (Figure 3.8**B**). There were no statistically significant differences between the means of the proportions of C1:fl between the cell lines as determined by one-way ANOVA ($F(3,12)=0.628$, $p=0.61$) (Figure 3.8**C**).

Together these data indicate that these mutant proteins are successfully processed through the ER and Golgi compartments resulting in mature PrP. Additionally, the presence of the C1 fragment after PNGase F digestion at equal levels compared to N2a cells indicates that α-cleavage processing is not affected by the amino acid substitutions or the introduction of the transgene into the genome.

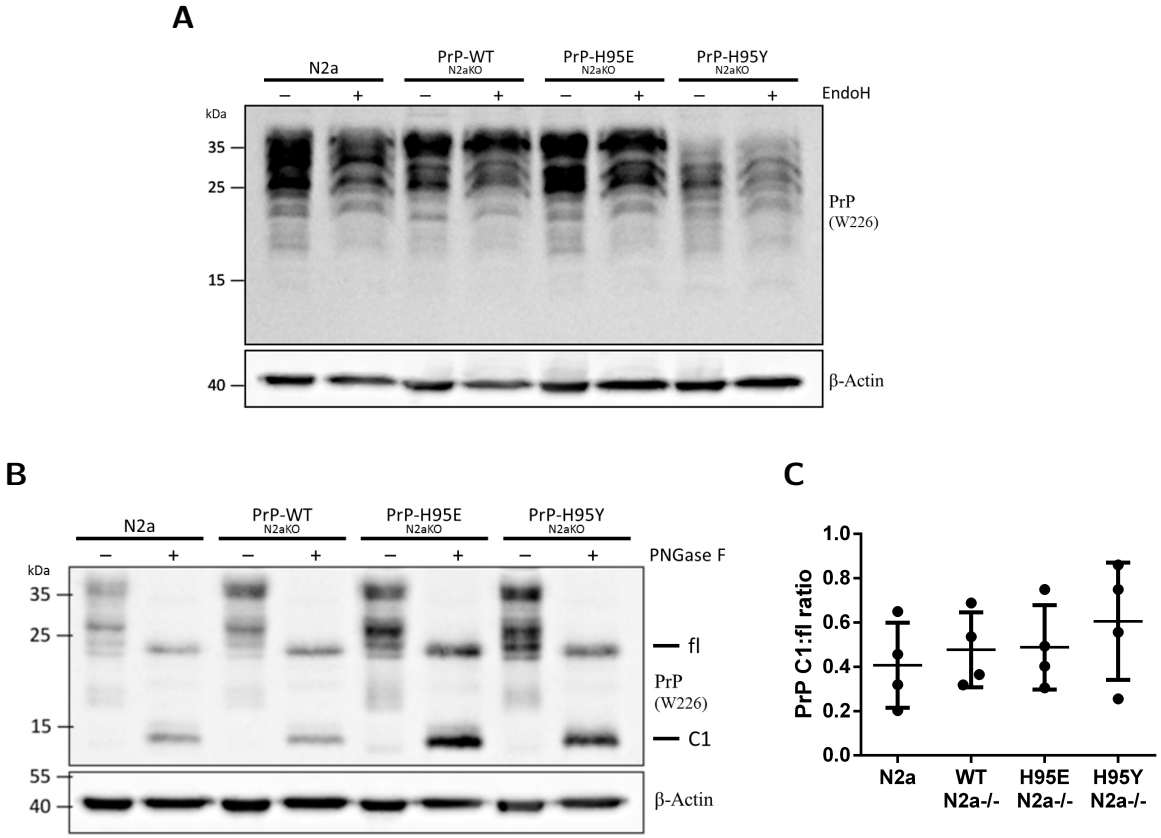

Figure 3.8: The H95 mutants share the same glycosylation patterns and proteolytic characteristics with PrP WT. (**A**) Thirty μg of either undigested cell lysates or digested with Endo H or (**B**) PNGase F. The full length PrP (fl) and C1 fragment (C1) are indicated. The positions of the diglycosylated (di), monoglycosylated (mono) and unglycosylated forms can be appreciated in the untreated lanes. PrP was detected by anti-PrP W226 antibody and B-actin was used as an internal loading control. (**C**) Quantitative analysis of the ratio of C1:fl after PNGase F digestion. n=4

3.4.3 Glycosidase digestion of ScN2a cells transiently transfected with PrP mutants with PNGase F revealed no differences of de-glycosylated patterns

We also digested samples of ScN2a cells transiently transfected with PrP WT_{3F4}, PrP $H95E_{3F4}$ and PrP $H95Y_{3F4}$ with PNGase F to compare the ratio of C1:C2 fragments, where an increase of C2 fragments is linked to prion disease. Unfortunately, the process of α-cleavage destroys the 3F4 epitope, so exogenous C1 fragments could not be visualized. We notice that the ratio of C2 fragment to full length protein is about 1:1 in all three cases (Figure 3.9).

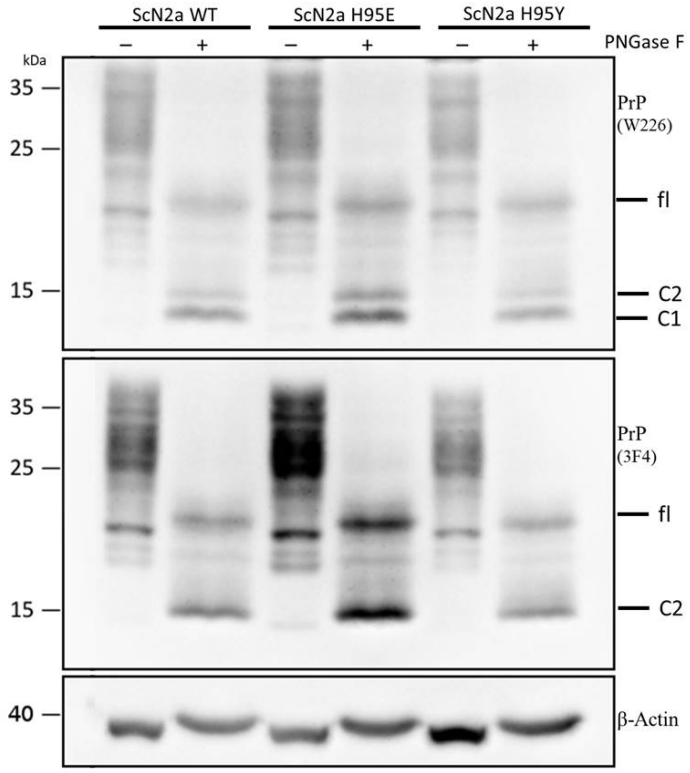

Figure 3.9: The H95 mutants transiently expressed in ScN2a cells share the same glycosylation patterns and proteolytic characteristics with PrP WT. Thirty μg of cell lysates from transiently transfected ScN2a were either undigested or digested by PNGase F were applied to each lane. The full length PrP (fl), C1 fragment (C1), and C2 fragment (C2) are indicated. The positions of the diglycosylated (di), monoglycosylated (mono) and unglycosylated forms can be appreciated in the untreated lanes. PrP was detected by anti-PrP W226 antibody for total PrP and anti-PrP 3F4 for exogenous, mutant PrP. B-actin was used as an internal loading control.

3.4.4 Solubility of PrP H95E and H95Y are unchanged

Solubility is an important biochemical property that differs between PrP^{Sc} and PrP^{C}. Soluble and insoluble PrP were separated by centrifugation at high speed. The resulting supernatant (soluble proteins) and pellet (insoluble proteins) were analyzed by Western Blot (Figure 3.10**A**). As expected, PrP of ScN2a cells contained a high amount of insoluble PrP (M=60.40%, SD=10.13). The rest of the cell lines examined contained roughly 20% insoluble PrP. PrP H95E and H95Y show slightly increased insolubility compared to WT, but very marginal (Figure 3.10**B**).

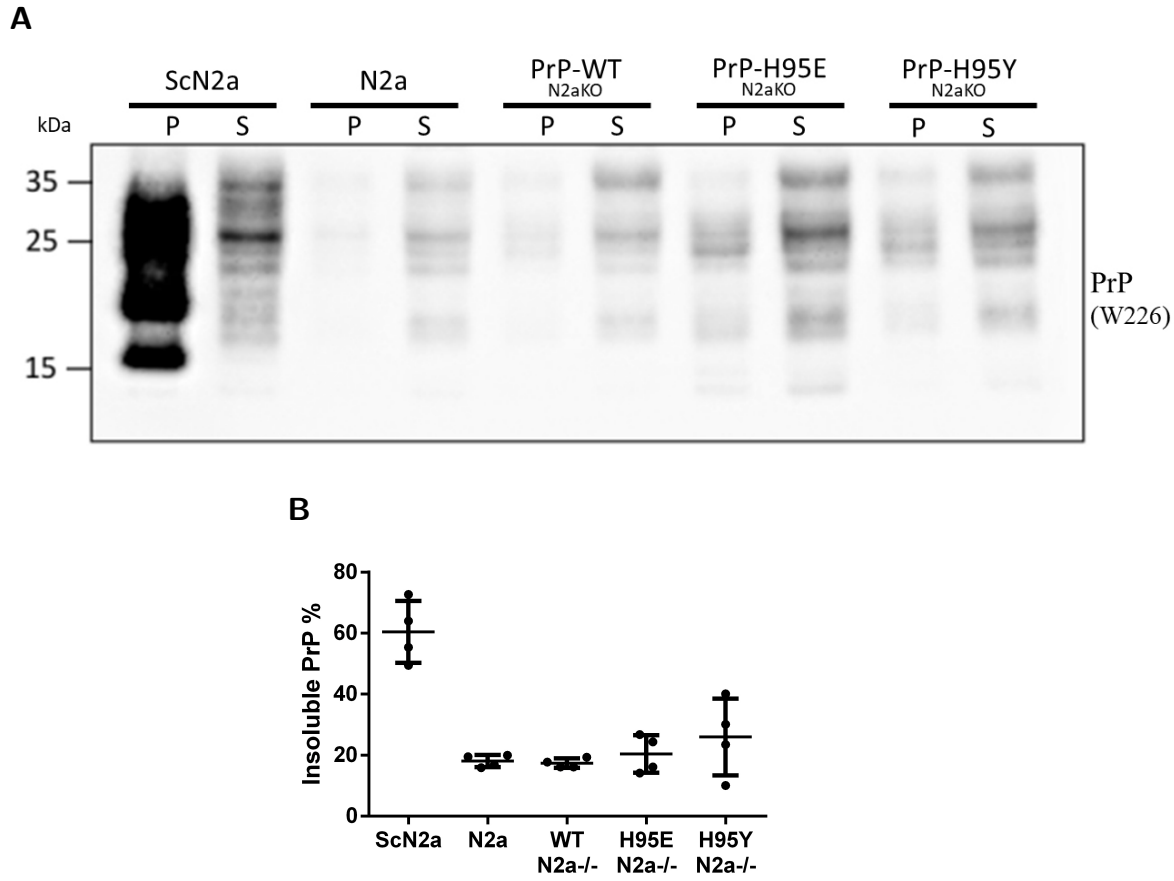

Figure 3.10: Solubility of mutant PrPs is slightly decreased. (**A**) Cell lysates from N2a PrP$-/-$ cells stably expressing PrP WT, PrP H95E and PrP H95Y were separated into supernatant (S) and pellet (P) fractions by 100,000 x g ultracentrifugation and subsequent washes. PrPs were detected by anti-PrP W226 antibody. (**B**) olubility profile for PrP of each cell line, percentage of insoluble PrP determined by the relative densitometry of the pellet signal relative to the total of the pellet and supernatant signal (n=4).

3.5 Localization and trafficking in N2aPrP−/− H95E, N2aPrP−/− H95Y cells

PrP WT, H95E and H95Y were stably expressed in N2a−/− cells and visualized by immunofluorescence to determine the localization of the WT and mutant PrPs. Compared to N2a cells endogenously expressing PrP, N2a−/− cell lines expressing WT, H95E and H95Y all had similar PrP distribution and localization: predominantly at the cell surface (Figure 3.11) with some intracellular localization as seen by the combined cell surface and intracellular staining of PrP in Figure 3.12.

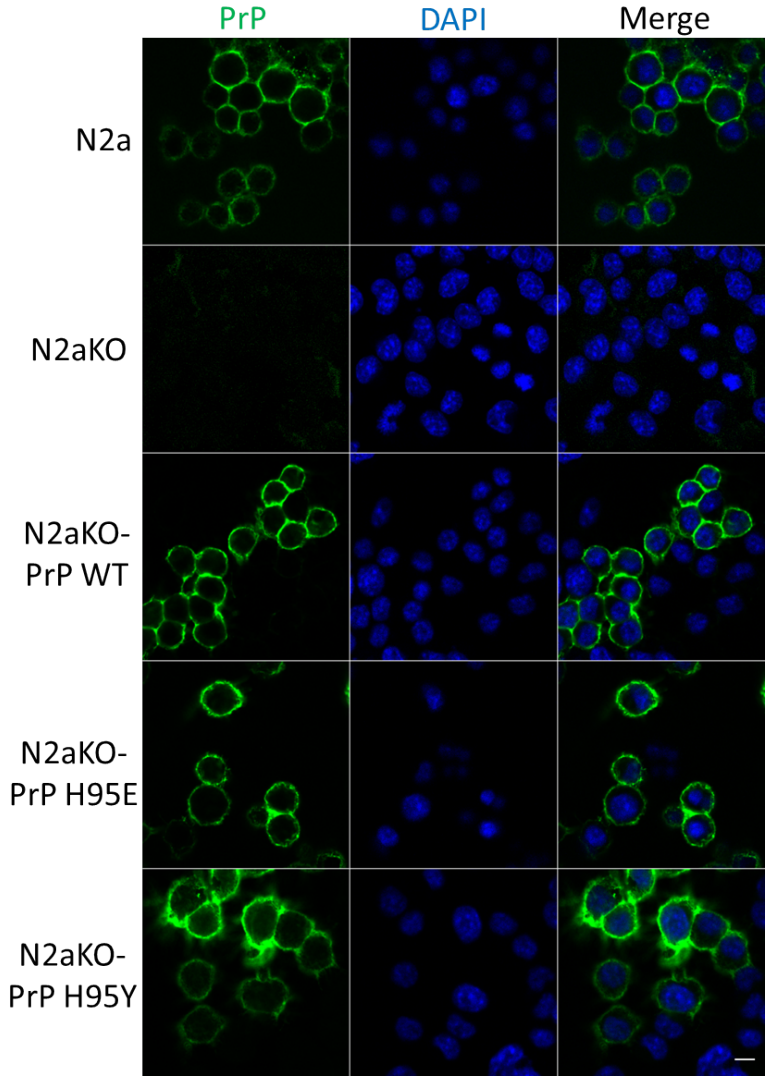

Figure 3.11: H95E and H95Y mutants are predominantly expressed on the cell surface, like WT PrP. Cell surface staining of N2a cells and stable transfection of PrP WT, H95E and H95Y in N2aKO cells. PrP on the cell surface was detected by anti-PrP W226 without permeabilization. PrP is in green, DAPI nuclear staining in blue, with merged images. Scale bar: 10 μm.

To further explore the subcellular localization and trafficking of PrP H95E and PrP H95Y, we analyzed the localization patterns of our mutants with respect to several organelle markers (Figure 3.12). All four of our cell lines analyzed, N2a, N2a$-/-$ PrP WT, N2a$-/-$ PrP H95E and N2a$-/-$ PrP H95Y continued to show prp mainly expressed at the cell surface. In the N2a and N2a$-/-$ PrP WT cell lines, prp localizes with EEA1 (early endosomal marker), Tfn (endosomal recycling compartment marker), LAMP1 (lysosomal marker); while there was no specific localization with M6PR (late endosome marker) or Calnexin (ER marker). Our mutant cell lines N2a$-/-$ PrP H95E and N2a$-/-$ PrP H95Y shared the same localization patterns as PrP WT in reference to the organelle markers, except for localization with the endosomal recycling compartment marker (Tfn). The WT PrP (of both N2a cells and N2a$-/-$ WT PrP) localize with Tfn as does PrP H95Y, though at a higher extent than WT PrP. However PrP H95E does not localize with Tfn. This difference of association with the endosomal recycling compartment marker, could affect the likelihood of PrP to misfold into PrP^{Sc}, as these mildly acidic compartments have been proposed as a likely site for prion conversion [129] [133] and pH has been found to have an effect on prion conversion propensity of PrP [73] [134].

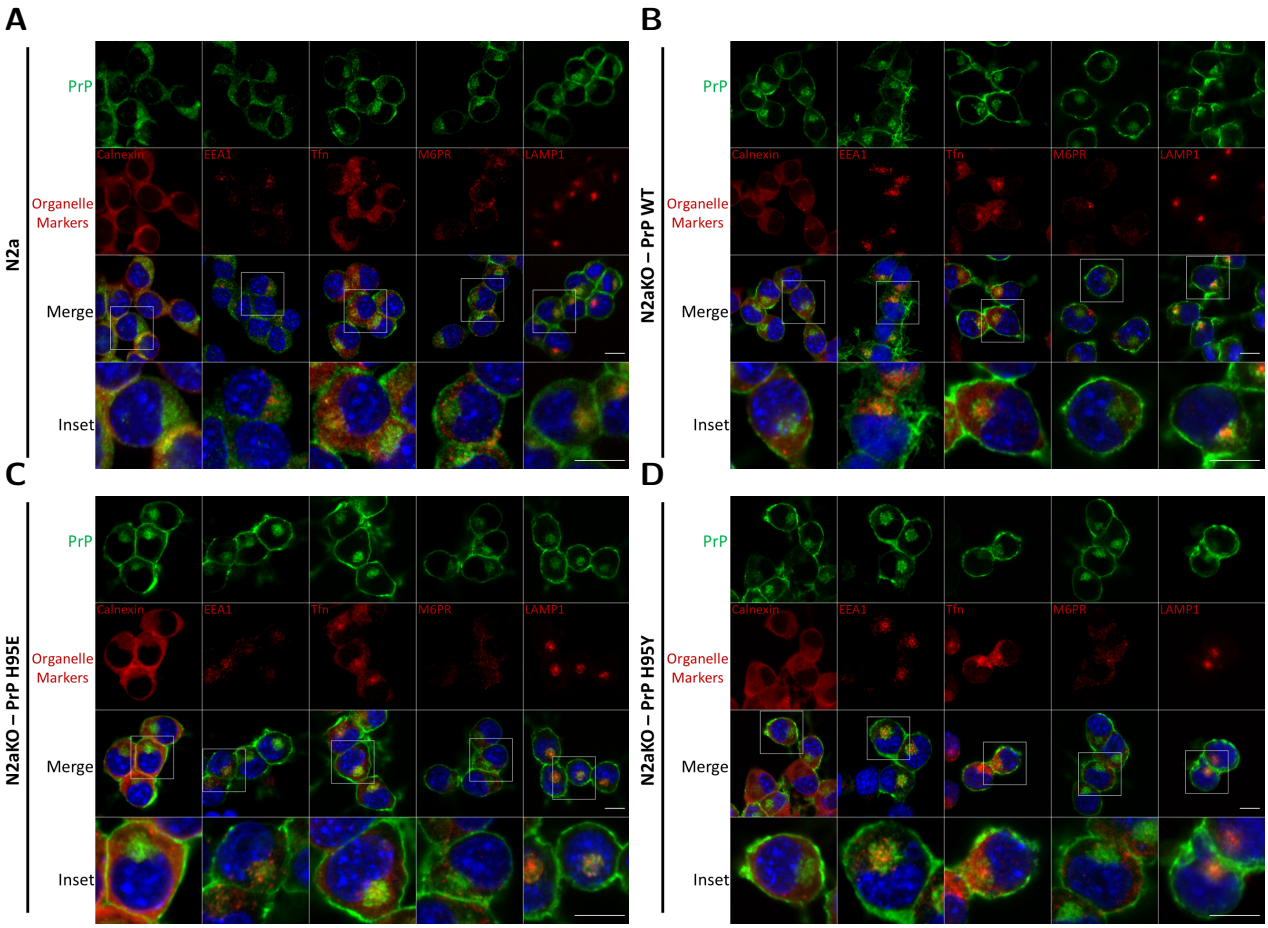

Figure 3.12: The H95E and H95Y mutants display altered localization patterns in the endosomal recycling compartments. (**A**) PrP localization in N2a cells (**B**), N2a PrP−/− WT PrP (**C**), N2a PrP−/− H95E (**D**) and N2a PrP−/− H95Y with reference to organelle markers. PrPs are detected by anti-PrP W226 antibody (green), nuclei are labeled with DAPI (blue) and organelle markers (red): Calnexin (ER marker), EEA1 (early endosome marker), Tfn (endosomal recycling compartment marker), M6PR (late endosome marker) and LAMP1 (lysosome marker). Insets show a magnification of the merged panels from white boxed areas. Scale bar: 10 μm.

3.6 Attempted establishment of Tg mice expressing MoPrP H95E

We used pJB1, a modified from MoPrP.Xho, as the vector to carry MoPrP H95E. This vector provides relatively high levels of transgene-encoded proteins in the brains and hearts of Tg Mice [5]. The MoPrP H95E coding sequence was inserted into pJB1, resulting in pJB::MoPrP(1-254, H95E). At the transgenic mouse facility of Cyagen Biosciences Inc (USA), the H95E mutant transgenes containing mouse regulatory sequences were excised from the plasmid and microinjected into the pronucleus of fertilized FVB mice eggs. Mice with transgene integration were screened by PCR using specific primers. Three F0 mice containing the transgene were identified and shipped to the animal facilities of Prof. Juan Maria Torres, INIA, Madrid, Spain. Here the mice were crossed with WT mice to obtain an F1 generation that was also screened using PCR amplification as above. Unfortunately, no F1 offspring containing the transgene were obtained (Figure 3.13).

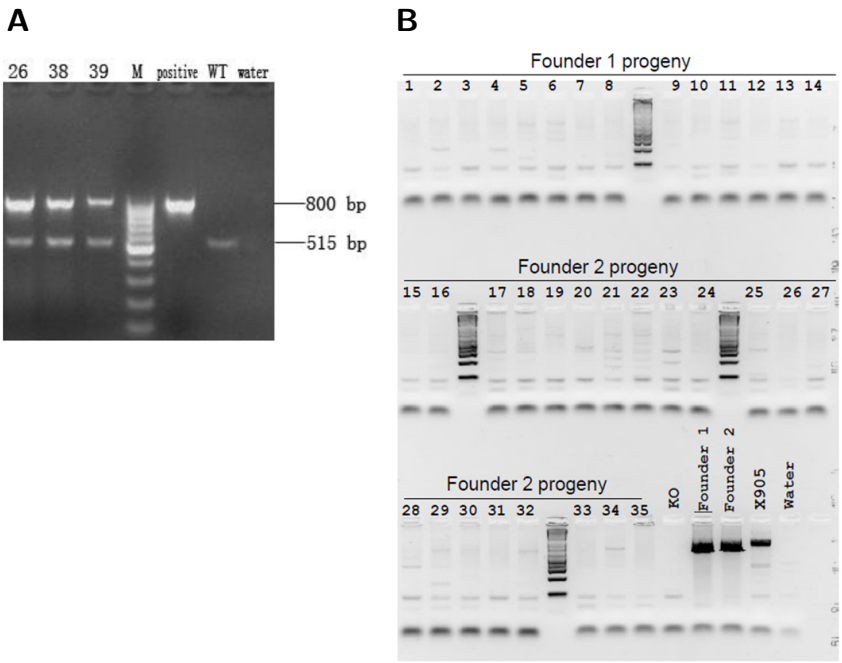

Figure 3.13: PCR assay for Tg mice screening. (**A**) PCR assay identifying three founders. Transgene PCR product size is 800 bp, internal control PCR product size is 515 bp. Positive control is 400 ng of mouse genomic DNA spikes with transgene injection DNA equal to 5 copies of transgene per diploid mouse genome. WT control is 400 ng of mouse genomic DNA. Water control is no DNA template added. (**B**) Representative PCR assay screening F1 mice. Transgene PCR product size is 800 bp. None of the progeny contained the transgene.

3.7 Expression and purification of recombinant PrP

MoPrP23-231 WT and MoPrP23-231 H95E were cloned into pET11a. These recombinant proteins were produced in E. coli Rosetta DE3 in LB medium. We show the results of MoPrP23-231 H95E here as a reference.

After induction with IPTG, MoPrP23-231 H95E was overexpressed in bacterial cells with clear band in SDS-PAGE (Figure 3.14**A**). MoPrP23-231 H95E was expressed in the bacteria as insoluble inclusion bodies, therefore they had to be solublized in 8M GdnHCl and purified under denaturing conditions. MoPrP23-231 H95E contains multiple Histidine regions in the N-terminal that can bind metals, such as copper, nickel and zinc. Relying on this characteristic, we first purified MoPrP23-231 H95E by Immobilized metal ion affinity chromatography (IMAC) by Histrap column. After this first purification, proteins were quite pure, with only a few contaminant bands. A second purification step of size exclusion chromatography (SEC) was performed to obtain highly purified proteins (Figure 3.14**B**). Protein purity and identity was confirmed by Ponceau stain and by Western blot with the W226 antibody (Figure 3.14**C** & 3.14**D**). These proteins will be used to analyze the kinetics of MoPrP23-231 H95E compared to MoPrP23-231 WT in fibrillization assay and RT-QuIC.

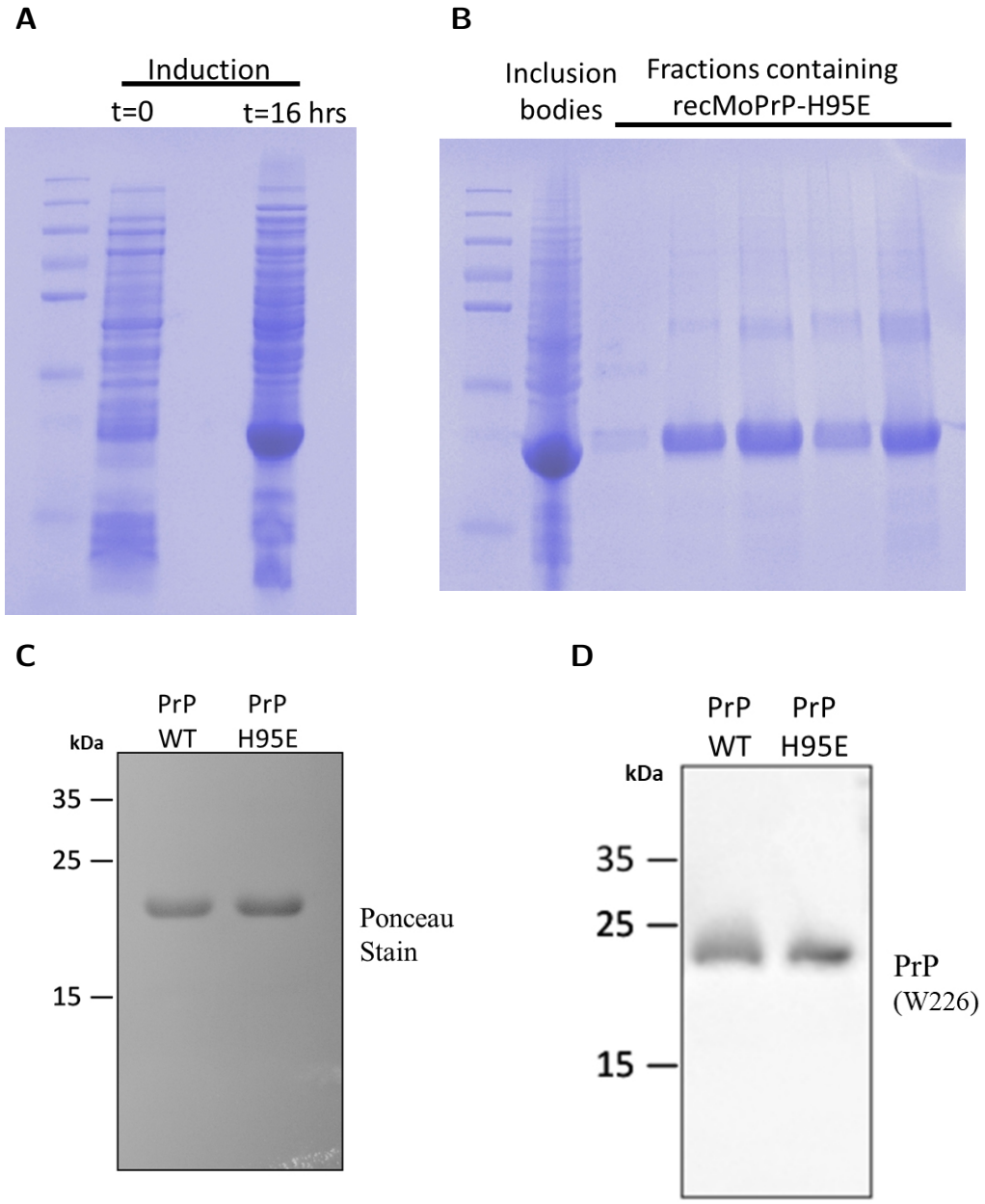

Figure 3.14: Expression and purification of MoPrP23-231 H95E. (**A**) Expression of MoPrP23-231 H95E in Rosetta DE3 bacteria before induction (t=0) and 16 hours after induction (t=16). (**B**) Purification of MoPrP23-231 H95E by Histrap column. (**C**) WB analysis of recombinant protein purity by Ponceau stain (**D**) and with anti-PrP W226 of both MoPrP23-231 WT and MoPrP23-231 H95E.

Chapter 4
4 Discussion

Prion diseases represent a poorly understood strain of neurodegenerative diseases with devastating effects to the brain. Understanding restraints and triggers of prion conversion, the predominant event of prion diseases leading to the propagation and infectivity of PrP^{Sc}, is crucial. Copper binding to PrP on the N-terminal,implicated in prion disease and conversion, might represent a key factor for such diseases.

4.1 Amino acid substitution H95 vastly changes prion conversion propensity

Previous work from our lab identified the non-OR histidine, the fifth of six copper binding histidines on PrP, as influential on prion conversion propensity, a fact observed when this histidine was substituted by the conservative mutation to tyrosine [73]. This study was the first to highlight the importance of this site in the conversion process. My colleagues reasoned from their work that it was most likely the absence of copper coordination at H95 that made PrP^{C} more susceptible to convert into PrP^{Sc} in acidic conditions.

Prompted by these results, we performed an amino acid scan at H95, replacing histidine with every other common amino acid. Remarkably, prion conversion propensity was vastly changed depending on the amino acid substitution at the site. The residues with hydrophobic side chains (V, F, Y, I, M, W, L) increased the prion conversion propensity, while the electrically charged side chains (D, E, K, R) decreased the prion conversion propensity.

As all of the substitutions removed the copper coordination ability at residue 95, but the prion conversion propensity increased, decreased or stayed the same, it is clear that simply the loss of copper binding at this site does not increase the protein's likelihood to convert to PrP^{Sc}.

4.2 Charged amino acids at H95 decrease prion conversion

We confirmed the previous results with substitutions that make PrP^{C} less susceptible to PrP^{Sc} conversion. Notably, all the amino acids changes which decrease prion conversion propensity are charged amino acids: both negative (glutamic acid and aspartic acid) and positive (arginine and lysine) (interestingly enough the final positively charged amino acid, histidine, is the native amino acid for this residue, though with a pKa of 6.7, it is often uncharged in physiological conditions). So, whereas one possible interpretation is that Giachin et al. are still correct overall in their findings, copper might not per se be the deciding factor, but rather the presence of a charge at this site which stabilizes the structure against conversion.

When a hydrophobic side chain is placed at this site the opposite effect is instead achieved. Hydrophobic side chains could increase the protein's likelihood to aggregate. The evidence for this is supported by the fact that due to thermodynamic pressure, hydrophobic aggregation can occur between two different polypeptide chains if two locally hydrophobic regions come into close contact in aqueous solution, forming amyloid fibrils and insoluble aggregates [91].As such when a charged side chain is present, the steric hindrance acts to hold the structure of this region in place, similarly to (or better than) copper coordination.

It would be interesting to develop other mutants of PrP based on these findings and observations, including the mutation of the other Histidine of the non-OR, both Histidines of the non-OR and/or mutating all of the histidines of the non-OR and OR region to glutamic acid (or another of the charged amino acids) to see the effect on prion conversion propensity. My findings and observations incline me to predict that mutating the other histidine of the non-OR region (residue H110) would have a similar effect on prion conversion propensity as the mutant at H95. However, this mutant might prevent the α cleavage processing of PrP, which could encourage more β-cleavage. Increased β-cleavage is linked to prion diseases so it's favoring could push the system to increased PrP^{Sc} production, regardless of the substituting amino acid.

Mutating both of the non-OR histidines to glutamic acid would also likely still reduce prion conversion potential structurally, but again α cleavage could be impaired, and with no copper binding abilities in the non-OR, functional properties of this mutant could be even more impaired. Finally, changing all of the histidines of the OR and non-OR region to glutamic acid would likely still reduce the protein's ability to convert to PrP^{Sc}, but not significantly. However, I would predict that it would be toxic to cell cultures as observed in *in vivo* studies removing all the copper-binding regions of

the N-terminal [88]. In the same manner, I would expect it to severely disrupt many physiological activities of PrP^C, specifically those which require copper binding ability. It might be the case that our mutant does not have so many negative effects on PrP copper-related function given that copper can still bind to the non-OR region via H110, and as such it would be interesting to test with some of the functions proposed for PrP^C.

4.3 Copper chelation mildly increases prion conversion propensity

We found that the removal of copper from the medium by cuprizone (CPZ) tended to increase the prion conversion propensity of PrP $H95E_{3F4}$ and PrP WT_{3F4}, but not significantly. This is in line with previous work in our lab [73], though they found a significant increase in prion conversion propensity in PrP WT_{3F4} when CPZ was added to the medium at the same concentration, in the same assay and the same cell line. The one change we could determine between the two experiments was the brand of fetal bovine serum (FBS) used and we reason that this might account for the differences seen. This highlights how delicate the influence of copper is on the prion conversion process and how copper studies involving PrP have been so conflicting to date, as even small changes in the system might have large implications on the results.

4.4 PrP H95E and PrP H95Y mutants behave biochemically very similar to PrP WT

α and β-cleavage processing in PrP H95E and PrP H95Y continues at levels similar to PrP WT. This makes it unlikely that an increase or decrease of PrP processing is the cause of differing levels of prion conversion. We showed that PrP H95E and PrP H95Y follow normal maturation through the ER and Golgi with glycosidase assays and are expressed at the cell surface at levels comparable to WT PrP. From the cell surface the mutant can be endocytosed to early endosomal compartments, but the fate of the mutant PrPs after this point could differ.

4.4.1 Potential role of the endosomal recycling compartment in mutant PrP conversion

We studied the localization of PrP H95E and PrP H95Y compared to WT PrP using immunofluorescence to mark various organelles. We found no differences between the localization characteristics of the mutant and WT PrPs with respect to EEA1 (early endosomal marker), LAMP1 (lysosomal marker), M6PR (late endosome marker) and Calnexin (ER marker). We did observe differences of localization patterns of PrPs compared to Tfn (endosomal recycling compartment marker), where PrP WT co-localizes, PrP H95Y co-localizes very strongly and PrP H95E does not co-localize with the endosomal recycling compartment (ERC). Therefore, it seems that the degree of PrP co-localization with the ERC is directly proportional to the prion conversion propensity of the PrP. This is supported by another work that found that PrP sorting to the endosomal recycling compartment is required for PrP^{Sc} production [129].

It would be interesting to test if blocking the movement of PrP from the early endosomes to the ERC in PrP H95Y and PrP H95E cells would cause a decrease in prion conversion. Of note, this method (overexpressing Rab22a) does not block early endosome to ERC trafficking in N2a cells, these experiments would need to be performed in GT1 cells. Results from this experiment could determine if the prion conversion propensity of PrP is more dependent on structure, to the intracellular compartments it is trafficked to or a combination of both.

Conflictingly, other work has showed that PrP internalization is not a requirement for prion conversion [50]. However, these data do not exclude a role for intracellular compartments in prion conversion, which may accelerate or spread the conversion and propagation of PrP^{Sc} after its initial conversion at the cell surface.

It is interesting to consider how the ERC might promote prion conversion. It has been suggested that the ERC allows for the close contact of many PrPs in a small space, accommodating conversion [129]. Or the slightly acidic environment of the ERCs (pH 6.4-6.5) [132] could favor a structural change of PrP since it has been shown that the mutant PrP H95Y is less stable than WT PrP at acidic conditions [73].

4.4.2 PK sensitive and infectious PrP^{Sc}

At this point we cannot rule out that the PrP H95E mutant produces PK-sensitive PrP^{Sc}. To understand this we are performing RT-QuIC and amyloid seeding assays. These assays will show if PrP H95E can convert into PrP^{Sc} in native conditions and denatured conditions, respectively, even if it is PK-sensitive. However, even if it can form

PrP^{Sc} in these assays, we cannot know if PrP^{Sc} of H95E is infective or disease-inducing. To answer these final questions we can first test *in vitro* using *de novo* scrapie infection assays in stably transfected N2a-/- PrP H95E cell lines. However, further *in vivo* experiments are necessary with Tg mice expressing PrP H95E to have a more complete picture of the possible infectious nature of PrP H95E.

We predict that mice expressing only the PrP H95E mutant would not show detrimental phenotypes since Tg mice expressing PrP H95Y [unpublished data, Legname lab] do not and our biochemical assays show similar behaviours of these two mutants. Also, due to the decreased prion conversion propensity observed in the prion conversion assays, we would expect that Tg mice expressing PrP H95E would not develop spontaneous prion disease and after scrapie inoculation would have lengthened survival times compared to WT mice.

4.4.3 Potential natural mutation of PrP H96Y in a human patient

When we began work on the H96 site H96 site (human numbering; mouse equivalent H95), we believed this to be a completely artificial mutation, however, we have found that a patient from Spain carried the PrP H96Y mutation and likely died of prion disease [28]. Unfortunately, an autopsy was not performed on this patient, so there is no confirmation of the diagnosis. Also, as far as we are aware, it is the only reported case of a natural mutation at this site. More information would be needed for any conclusions to be drawn, but it is tempting to fit this with our experimental data, where we find in *in vitro* and in *in vivo* mice experiments that this mutation causes an increase in PrP^{Sc} formation.

4.5 Future directions for this project

Currently we are performing RT-QuIC and amyloid seeding assays to determine the *in vitro* protein kinetics of PrP H95E compared to PrP WT. We are also finishing the *de novo* scrapie infections of stably transfected N2a-/- PrP H95E cell lines. Next, *in vivo* experiments are crucial and indispensable in order to asses the validity of the results of *in vitro* experiments. The information extracted from *in vivo* experiments is fundamental to support the relevance in live animals, a much more complicated system than *in vitro* systems can replicate. The H95E mice generated did not transmit the transgene to their offspring. We cannot explain why this occurred as we have no reason to infer that PrP H95E would be toxic. Tg mice expressing PrP H95Y survive and

transmit the transgene as expected. Structural studies by XFAS on PrP H95E would be very interesting as they might shed light into the conformational properties that play a role in the conversion process. In line with the results obtained by my colleagues on the H95Y mutant, we would likely find that the PrP H95E mutant maintains the more stable conformation in both acidic and physiological conditions, even though it is unable to coordinate copper at residue 95.

4.6 Conclusions

These data reaffirm the hypothesis that the non-OR region of PrP is involved in prion conversion, but now we can add that it is involved in both increased and decreased prion conversion propensities.

The opportunity of finding the key mutations in PrP that might lead to a controlled tool for prion disease sequestering is now bigger than ever. The continuous detailed studies performed by my colleagues and I at Legname's lab are a strong indication of fruitful and possibly game-changing research in the prion field. The discovery of mutants, such as the ones presented in this thesis, which might prove reduced conversion propensity into PrP^{Sc} is an exciting path to pursue. If the confirmation of these results *in vivo*, with zero or minimal negative effects on physiological function are confirmed, then the usability of this to create prion-resistant animals would represent a unique possibility.

The research presented here will help us understand in a deeper way the mechanisms involved in prion conversion and the players involved in such a delicate and poorly understood process, which is a key element in prion diseases.

Acknowledgements

A PhD is an adventure of unexpected proportions, I can say that now with full knowledge. My arrival at SISSA was met by a curious discovery of people and new customs, along with the characteristic lab that I spent the last years of my life working at, I was so excited and thankful to be here.

There are many names I will not be able to mention here, but they know who they are. For every little favour and talk, for every time you took care of my rabbits so I could keep working. To all of you, thank you.

I will always be grateful to SISSA and Trieste in general, for the way everyone treated me during my maternity leave. I want to mention my supervisor Giuseppe Legname, whose support during that time made things much easier to deal with. Never was I in distress because of the way my work and my personal life interfered with one another.

I want to thank my parents as well, for their support was unfaltering and reassuring, I would not have been able to do this without you. Additionally to my parents-in-law who were also willing to make the long journey to help me, at often a moment's notice.

My husband, Alejandro, always there, always willing. To you I want to thank you for the uncountable hours talking, the time spent helping me and holding me so I would not fall.

And finally I want to thank my son, Ezio, for he is the source of my happiness, the light of my life, my cute baby. The one that makes everything worth it, every long night and hard discussion. All the sweat and all the tears that came, for him I would do it all again.

Bibliography

[1] Taraboulos, A., D. Serban, and S.B. Prusiner, Scrapie prion proteins accumulate in the cytoplasm of persistently infected cultured cells. J Cell Biol. 1990;110(6):2117-32.

[2] Kaneko, K., et al., Evidence for protein X binding to a discontinuous epitope on the cellular prion protein during scrapie prion propagation. Proc Natl Acad Sci U S A. 1997; 94(19):10069-74.

[3] Kascsak, R.J., et al., Mouse polyclonal and monoclonal antibody to scrapie-associated fibril proteins. J Virol. 1987;61(12):3688-93.

[4] Maley, F., et al., Characterization of glycoproteins and their associated oligosaccharides through the use of endoglycosidases. Anal Biochem, 1989;180(2):195-204.

[5] Borchelt, D.R., et al., A vector for expressing foreign genes in the brains and hearts of transgenic mice. Genet Anal. 1996;13(6):159-63.

[6] Mehrabian, M., et al., CRISPR-Cas9-based knockout of the prion protein and its effect on the proteome. PLoS One. 2014;9(12):E114594.

[7] Herbert Budka. Neuropathology of prion diseases. British Medical Bulletin. 2003;66(1):121-130.

[8] Geschwind, M.D. Prion Diseases. Continuum (Minneap Minn). 2015 Dec;21(6 Neuroinfectious Disease):1612-1638.

[9] Schatzl, H.M., et al. Prion protein gene variation among primates. J Mol Biol. 1995;245(4):362-74.

[10] Acevedo-Morantes, C.Y. & Wille, H. The Structure of Human Prions: From Biology to Structural Models â Considerations and Pitfalls. Viruses. 2014;6(10):3875-3892.

[11] Liang J. & Kong Q. alpha-cleavage of cellular prion protein. Prion. 2012;6(5):453-460.

[12] Orru C.D, et al. A Test for Creutzfeldt-Jakob Disease Using Nasal Brushings. N Engl J Med. 2014;371:519-529.

[13] Linden, R., et al. Physiology of the prion protein. Physiol Rev. 2008;88(2):673-728.

[14] Taylor DR, Hooper NM. The prion protein and lipid rafts. Mol Membr Biol. 2006;23:89-99

[15] Collinge, J., Human prion diseases and bovine spongiform encephalopathy (BSE). Hum. Mol. Genet.1997;6:1699-1705.

[16] Aguzzi, A. et al., Insights into prion strains and neurotoxicity. Nat. Rev. Mol. Cell Biol. 2007;8:552-561

[17] Sigurdson, C.J. et al., Prion strain discrimination using luminescent conjugated polymers. Nat. Methods. 2007;4:1023-1030

[18] Prusiner, S.B., Scrapie prions, brain amyloid, and senile dementia. Curr. Top. Cell. Regul. 1985;26:79-95

[19] Wulf, M., Senatore, A.,Aguzzi, A. The biological function of the cellular prion protein: an update. BMC Biology. 2017;15:34

[20] Harris DA, Huber MT, Van Dijken P, Shyng SL, Chait BT, Wang R. Processing of a cellular prion protein: identification of N-and C-terminal cleavage sites. Biochemistry (Mosc). 1993;32:1009-16.

[21] Walmsley AR, Watt NT, Taylor DR, Perera WSS, Hooper NM. α-cleavage of the prion protein occurs in a late compartment of the secretory pathway and is independent of lipid rafts. Mol Cell Neurosci. 2009;40:242-8.

[22] Chen SG, Teplow DB, Parchi P, Teller JK, Gambetti P, Autilio-Gambetti L. Truncated forms of the human prion protein in normal brain and in prion diseases. J Biol Chem. 1995;270:19173-80.

[23] Lewis V, Johanssen VA, Crouch PJ, Klug GM, Hooper NM, Collins SJ. Prion protein "gamma-cleavage": characterizing a novel endoproteolytic processing event. Cell Mol Life Sci. 2016;73:667-83.

[24] Westergard L, Turnbaugh JA, Harris DA. A naturally occurring C-terminal fragment of the prion protein (PrP) delays disease and acts as a dominant-negative inhibitor of PrPSc formation. J Biol Chem. 2011;286:44234-42.

[25] Yusa S, Oliveira-Martins JB, Sugita-Konishi Y, Kikuchi Y. Cellular prion protein: from physiology to pathology. Viruses. 2012;4:3109-31.

[26] Bendheim PE, Brown HR, Rudelli RD, Scala LJ, Goller NL, Wen GY, et al. Nearly ubiquitous tissue distribution of the scrapie agent precursor protein. Neurology. 1992;42:149.

[27] Nuvolone M, Hermann M, Sorce S, Russo G, Tiberi C, Schwarz P, et al. Strictly co-isogenic C57BL/6 J- Prnp $-/-$ mice: A rigorous resource for prion science. J Exp Med. 2016;213:313-27.

[28] Minikel EV, Vallabh SM, Lek M, Estrada K, Samocha KE, Sathirapongsasuti JF, et al. Quantifying prion disease penetrance using large population control cohorts. Sci Transl Med. 2016;8:322ra9.

[29] Colby, D.W., et al., Prion detection by an amyloid seeding assay. Proc Natl Acad Sci USA. 2007;104(52):20914-9.

[30] Lund, C. et al. Characterization of the Prion Protein 3F4 Epitope and Its Use as a Molecular Tag. J Neurosci Methods. 2007;165(2):183-190.

[31] Prusiner, S.B. Molecular biology of prion diseases. Science. 1991;252(5012):1515-22.

[32] Prusiner, S.B. Novel proteinaceous infectious particles cause scrapie. Science. 1982;216:136-144.

[33] Soto, C. Prion hypothesis: the end of the controversy? Trends Biochem Sci. 2011 Mar;36(3):151-8.

[34] Legname G, Baskakov IV, Nguyen HO, Riesner D, Cohen FE, DeArmond SJ, Prusiner SB. Synthetic mammalian prions. Science. 2004;305(5684):673-6.

[35] Makarava N, Kovacs GG, Bocharova O, Savtchenko R, Alexeeva I, Budka H, Rohwer RG, Baskakov. Recombinant prion protein induces a new transmissible prion disease in wild-type animals. IV Acta Neuropathol. 2010;119(2):177-87.

[36] Kim JI, Cali I, Surewicz K, Kong Q, Raymond GJ, Atarashi R, Race B, Qing L, Gambetti P, Caughey B, Surewicz WK. Mammalian prions generated from bacterially expressed prion protein in the absence of any mammalian cofactors. J Biol Chem. 2010;285(19):14083-7.

[37] Wang F, Wang X, Yuan CG, Ma. Generating a prion with bacterially expressed recombinant prion protein. J Science. 2010;327(5969):1132-5.

[38] Holmes BB, Diamond MI. Prion-like properties of Tau protein: the importance of extracellular Tau as a therapeutic target. J Biol Chem. 2014;289(29):19855-61.

[39] Ashe KH, Aguzzi A. Prions, prionoids and pathogenic proteins in Alzheimer disease. Prion. 2013;7(1):55-9.

[40] Prusiner S. B. A unifying role for prions in neurodegenerative diseases. Science. 2012;336:1511-1513

[41] Halfmann R, Alberti S, Lindquist S. Prions, protein homeostasis, and phenotypic diversity. Trends Cell Biol. 201;20(3):125-33.

[42] Sanders, D.W. et al. Distinct tau prion strains propagate in cells and mice and define different tauopathies. Neuron. 2014;82:1271-1288

[43] Lu, J.X. et al. Molecular structure of beta-amyloid fibrils in Alzheimer's disease brain tissue. Cell. 2013;154:1257-1268

[44] Simoneau, S. et al. In vitro and in vivo neurotoxicity of prion protein oligomers. PLoS Pathog. 2007;3:e125

[45] Brandner, S. et al. Normal host prion protein necessary for scrapie-induced neurotoxicity. Nature. 1996;379:339-343

[46] Huotari, J. and Helenius, A. Endosome maturation. EMBO J. 2011;30:3481-3500

[47] Yim, Y.I. et al. The multivesicular body is the major internal site of prion conversion. J. Cell Sci. 2015;128:1434-1443

[48] Goold, R. et al. Alternative fates of newly formed PrPSc upon prion conversion on the plasma membrane. J. Cell Sci. 2013;126:3552-3562

[49] Rouvinski, A. et al. Live imaging of prions reveals nascent PrPSc in cell-surface, raft-associated amyloid strings and webs. J. Cell Biol. 2014;204:423-441

[50] Goold, R. et al. Rapid cell-surface prion protein conversion revealed using a novel cell system. Nat. Commun. 2011;2:281

[51] Brown DR, Clive C, Haswell SJ. Antioxidant activity related to copper binding of native prion protein. J Neurochem. 2001;76:69-76.

[52] Taylor DR, Parkin ET, Cocklin SL, Ault JR, Ashcroft AE, Turner AJ, et al. Role of ADAMs in the ectodomain shedding and conformational conversion of the prion protein. J Biol Chem. 2009;284:22590-600.

[53] Vincent B, Paitel E, Saftig P, Frobert Y, Hartmann D, De Strooper B, et al. The disintegrins ADAM10 and TACE contribute to the constitutive and phorbol ester-regulated normal cleavage of the cellular prion protein. J Biol Chem. 2001;276:37743-6.

[54] Altmeppen HC, Prox J, Puig B, Kluth MA, Bernreuther C, Thurm D, et al. Lack of a-disintegrin-and-metalloproteinase ADAM10 leads to intracellular accumulation and loss of shedding of the cellular prion protein in vivo. Mol Neurodegener. 2011;6:36.

[55] Altmeppen HC, Prox J, Krasemann S, Puig B, Kruszewski K, Dohler F, et al. The sheddase ADAM10 is a potent modulator of prion disease. Elife. 2015;4, e04260.

[56] Gambetti, P., et al., A novel human disease with abnormal prion protein sensitive to protease. Ann Neurol. 2008;63(6): 697-708.

[57] Gasset, M., et al. Perturbation of the secondary structure of the scrapie prion protein under conditions that alter infectivity. Proc Natl Acad Sci USA. 1993;90(1):1-5.

[58] Vazquez-Fernandez E, Vos MR, Afanasyev P, Cebey L, Sevillano AM, Vidal E, Rosa I, Renault L, Ramos A, Peters PJ, FernÃ¡ndez JJ, van Heel M, Young HS, Requena JR, Wille H PLoS Pathog. The Structural Architecture of an Infectious Mammalian Prion Using Electron Cryomicroscopy. 2016;12(9):e1005835.

[59] Wille H, Bian W, McDonald M, Kendall A, Colby DW, Bloch L, Ollesch J, Borovinskiy AL, Cohen FE, Prusiner SB, Stubbs G. Natural and synthetic prion structure from X-ray fiber diffraction. Proc Natl Acad Sci USA. 2009 Oct 6; 106(40):16990-5.

[60] T.P. Knowles, C.A. Waudby, G.L. Devlin, S.I. Cohen, A. Aguzzi, M. Vendruscolo, E.M. Terentjev, M.E. Welland, C.M. Dobson. An analytical solution to the kinetics of breakable filament assembly. Science. 2009;326:1533-1537.

[61] J.S. Griffith. Self-replication and scrapie. Nature. 1967;215:1043-1044.

[62] S.B. Prusiner. Prions. Proc. Natl. Acad. Sci. U. S. A. 1998;95:13363-13383.

[63] J.T. Jarrett, P.T. Lansbury. Seeding "one-dimensional crystallization" of amyloid: a pathogenic mechanism in Alzheimer's disease and scrapie?. Cell. 1993;73:1055-1058.

[64] D.C. Gajdusek. Transmissible and non-transmissible amyloidoses: autocatalytic post-translational conversion of host precursor proteins to beta-pleated sheet configurations. J. Neuroimmunol. 1988;20:95-110.

[65] Aronoff-Spencer, E., et al., Identification of the Cu2+ binding sites in the N-terminal domain of the prion protein by EPR and CD spectroscopy. Biochemistry. 2000;39(45):13760-71.

[66] Burns, C.S., et al. Molecular features of the copper binding sites in the octarepeat domain of the prion protein. Biochemistry. 2002;41(12):3991-4001.

[67] Kim Y, Lee J, Lee C. In silico comparative analysis of DNA and amino acid sequences for prion protein gene. Transbound Emerg Dis. 2008;55(2):105-14.

[68] Zahn, R. et al. NMR solution structure of the human prion protein. Proc Natl Acad Sci USA. 2000;97:145-150.

[69] Surewicz, W. K.& Apostol, M. I. Prion protein and its conformational conversion: a structural perspective. Top Curr Chem. 2011;305:135-167.

[70] Walter, E. D., Chattopadhyay, M.& Millhauser, G. L. The affinity of copper binding to the prion protein octarepeat domain: evidence for negative cooperativity. Biochemistry. 2006;45:13083-13092.

[71] Walter, E. D. et al. Copper binding extrinsic to the octarepeat region in the prion protein. Curr Protein Pept Sci. 2009;10:529-535.

[72] Jobling, M. F. et al. The hydrophobic core sequence modulates the neurotoxic and secondary structure properties of the prion peptide 106-126. J Neurochem. 1999;73:1557-1565.

[73] Gabriele Giachin, Phuong Thao Mai, Thanh Hoa Tran, Giulia Salzano, Federico Benetti, Valentina Migliorati, Alessandro Arcovito, Stefano Della Longa, Giordano Mancini, Paola D'Angelo, Giuseppe Legname. The non-octarepeat copper binding site of the prion protein is a key regulator of prion conversion Scientific Reports. 2015;5:15253.

[74] Caiati, M. D. et al. PrPC controls via protein kinase A the direction of synaptic plasticity in the immature hippocampus. J Neurosci. 2013;33:2973-2983.

[75] Steele, A. D., Emsley, J. G., Ozdinler, P. H., Lindquist, S.& Macklis, J. D. Prion protein (PrPc) positively regulates neural precursor proliferation during developmental and adult mammalian neurogenesis. Proc Natl Acad Sci USA 2006;103:3416-3421.

[76] Santuccione, A., Sytnyk, V., Leshchyns'ka, I.& Schachner, M. Prion protein recruits its neuronal receptor NCAM to lipid rafts to activate p59fyn and to enhance neurite outgrowth. J Cell Biol. 2005;169:341-354.

[77] Gasperini, L., Meneghetti, E., Pastore, B., Benetti, F.& Legname, G. Prion Protein and Copper Cooperatively Protect Neurons by Modulating NMDA Receptor Through S-nitrosylation. Antioxidants& Redox Signaling. 2014;22:772-784.

[78] Khosravani, H. et al. Prion protein attenuates excitotoxicity by inhibiting NMDA receptors. J Cell Biol 2008;181:551-565.

[79] Stys, P. K., You, H.& Zamponi, G. W. Copper-dependent regulation of NMDA receptors by cellular prion protein: implications for neurodegenerative disorders. J Physiol. 2012;590:1357-1368.

[80] Pushie, M. J. et al. Prion protein expression level alters regional copper, iron and zinc content in the mouse brain. Metallomics. 2011;3:206-214.

[81] Walter, E. D., Stevens, D. J., Visconte, M. P.& Millhauser, G. L. The prion protein is a combined zinc and copper binding protein: Zn2+ alters the distribution of Cu2+ coordination modes. J Am Chem Soc. 2007;129:15440-15441.

[82] Pauly, P.C. and D.A. Harris, Copper stimulates endocytosis of the prion protein. J Biol Chem. 1998;273(50):33107-10.

[83] Perera, W.S. and N.M. Hooper. Ablation of the metal ion-induced endocytosis of the prion protein by disease-associated mutation of the octarepeat region. Curr Biol. 2001;11(7):519-23.

[84] Fischer, M. et al. Prion protein (PrP) with amino-proximal deletions restoring susceptibility of PrP knockout mice to scrapie. EMBO J. 1996;15:1255-1264.

[85] Abskharon, R. N. et al. Probing the N-terminal beta-sheet conversion in the crystal structure of the human prion protein bound to a nanobody. J Am Chem Soc. 2014;136:937-944.

[86] Younan, N. D. et al. Copper(II)-induced secondary structure changes and reduced folding stability of the prion protein. J Mol Biol. 2011;410, 369-382.

[87] Migliorini, C., Sinicropi, A., Kozlowski, H., Luczkowski, M.& Valensin, D. Copper-induced structural propensities of the amyloidogenic region of human prion protein. J Biol Inorg Chem. 2014;19:635-645.

[88] Baumann, F. et al. Lethal recessive myelin toxicity of prion protein lacking its central domain. EMBO J. 2007;26:538-547.

[89] Li, A. et al. Neonatal lethality in transgenic mice expressing prion protein with a deletion of residues 105-125. EMBO J. 2007;26:548-558.

[90] Shmerling D, Hegyi I, Fischer M, BlÃ€ttler T, Brandner S, GÃ¶tz J, RÃŒlicke T, Flechsig E, Cozzio A, von Mering C, Hangartner C, Aguzzi A, Weissmann C. Expression of amino-terminally truncated PrP in the mouse leading to ataxia and specific cerebellar lesions. Cell. 1998; 93(2):203-14.

[91] Protein misfolding and aggregation: new examples in medicine and biology of the dark side of the protein world Massimo Stefani https://doi.org/10.1016/j.bbadis.2004.08.004

[92] Toni, M., et al. Extracellular copper ions regulate cellular prion protein (PrPC) expression and metabolism in neuronal cells. FEBS Lett. 2005;579(3):741-4.

[93] Varela-Nallar, L., et al. Induction of cellular prion protein gene expression by copper in neurons. Am J Physiol Cell Physiol. 2006;290(1):271-81.

[94] Herms, J., et al. Evidence of presynaptic location and function of the prion protein. J Neurosci. 1999;19(20):8866-75.

[95] Kretzschmar, H.A., et al. Function of PrP(C) as a copper-binding protein at the synapse. Arch Virol Suppl. 2000;16:239-49.

[96] Kralovicova, S., et al. The effects of prion protein expression on metal metabolism. Mol Cell Neurosci. 2009;41(2):135-47.

[97] Brown D.R.Prion protein expression modulates neuronal copper content J. Neurochem. 2003;87:377-385

[98] Brown D.R., Schmidt B., Kretzschmar H.A. Expression of prion protein in PC12 is enhanced by exposure to oxidative stress. Int. J. Dev. Neurosci. 1997;15:961-972.

[99] Pauly, P.C. and D.A. Harris. Copper stimulates endocytosis of the prion protein. J Biol Chem. 1998;273(50):33107-10.

[100] Kimberlin, R.H. and G.C. Millson. The effects of cuprizone toxicity on the incubation period of scrapie in mice. J Comp Pathol. 1976;86(3):489-96.

[101] Orem, N.R., et al. Copper (II) ions potently inhibit purified PrPres amplification. J Neurochem. 2006;96(5):1409-15.

[102] Bocharova, O.V., et al. Copper(II) inhibits in vitro conversion of prion protein into amyloid fibrils. Biochemistry. 2005:44(18):6776-87.

[103] Hijazi, N., et al. Copper binding to PrPC may inhibit prion disease propagation. Brain Res. 2003;993(1-2):192-200.

[104] Mitteregger, G., et al. Role of copper and manganese in prion disease progression. Brain Res. 2009;1292:155-64.

[105] Flechsig, E., et al. Prion protein devoid of the octapeptide repeat region restores susceptibility to scrapie in PrP knockout mice. Neuron. 2000;27(2):399-408.

[106] Goldfarb LG, Brown P, McCombie WR, Goldgaber D, Swergold GD, Wills PR, Cervenakova L, Baron H, Gibbs CJ Jr, Gajdusek DC. Transmissible familial Creutzfeldt-Jakob disease associated with five, seven, and eight extra octapeptide coding repeats in the PRNP gene. Proc Natl Acad Sci U S A. 1991;88(23):10926-30.

[107] Beck JA, Mead S, Campbell TA, Dickinson A, Wientjens DP, Croes EA, Van Duijn CM, Collinge. Two-octapeptide repeat deletion of prion protein associated with rapidly progressive dementia. J. Neurology. 2001;57(2):354-6.

[108] Owen, F., et al. Insertion in prion protein gene in familial Creutzfeldt-Jakob disease. Lancet. 1989;1(8628):51-2.

[109] Sigurdsson, E.M., et al. Copper chelation delays the onset of prion disease. J Biol Chem. 2003;278(47):46199-202.

[110] Mayer ML. Structural biology of glutamate receptor ion channel complexes. Curr Opin Struct Biol. 2016;41:119-27.

[111] Khosravani H, Zhang Y, Tsutsui S, Hameed S, Altier C, Hamid J, et al. Prion protein attenuates excitotoxicity by inhibiting NMDA receptors. Sci Signal. 2008;181:551.

[112] Gadotti VM, Bonfield SP, Zamponi GW. Depressive-like behaviour of mice lacking cellular prion protein. Behav Brain Res. 2012;227:319-23.

[113] Gadotti VM, Zamponi GW. Cellular prion protein protects from inflammatory and neuropathic pain. Mol Pain. 2011;7:1.

[114] You H, Tsutsui S, Hameed S, Kannanayakal TJ, Chen L, Xia P, et al. A neurotoxicity depends on interactions between copper ions, prion protein, and N-methyl-D-aspartate receptors. Proc Natl Acad Sci U S A. 2012;109:1737-42.

[115] Gasperini L, Meneghetti E, Pastore B, Benetti F, Legname G. Prion protein and copper cooperatively protect neurons by modulating NMDA receptor through S-nitrosylation. Antioxid Redox Signal. 2015;22:772-84.

[116] BÃŒeler H, Aguzzi A, Sailer A, Greiner RA, Autenried P, Aguet M, Weissmann C. Mice devoid of PrP are resistant to scrapie. Cell. 1993;73(7):1339-47.

[117] Stahl N, Borchelt DR, Hsiao K, Prusiner SB. Scrapie prion protein contains a phosphatidylinositol glycolipid. Cell. 1987;51:229-40.

[118] Stahl N, Baldwin M, Hecker R, Pan K-M, Burlingame A, Prusiner S. Glycosylinositol phospholipid anchors of the scrapie and cellular prion proteins contain sialic acid. Biochemistry (Mosc). 1992;31:5043-53.

[119] Naslavsky N, Stein R, Yanai A, Friedlander G, Taraboulos A. Characterization of detergent-insoluble complexes containing the cellular prion protein and its scrapie isoform. J Biol Chem. 1997;272:6324-31.

[120] Morris RJ, Parkyn CJ, Jen A. Traffic of prion protein between different compartments on the neuronal surface, and the propagation of prion disease. FEBS Lett. 2006;580:5565-71.

[121] Parizek P. Similar turnover and shedding of the cellular prion protein in primary lymphoid and neuronal cells. J Biol Chem. 2001;276:44627-32.

[122] Turk E, Teplow DB, Hood LE, Prusiner SB. Eur J Biochem. Purification and properties of the cellular and scrapie hamster prion proteins. 1988;176(1):21-30.

[123] Hebert DN, Molinari M. In and out of the ER: protein folding, quality control, degradation, and related human diseases. Physiol Rev. 2007;87(4):1377-408.

[124] Hudson H. Freeze and Christian Kranz Endoglycosidase and Glycoamidase Release of N-Linked Glycans Curr Protoc Mol Biol. 2010;17.

[125] Eigen M. Prionics or the kinetic basis of prion diseases. Biophys Chem. 1996;10(63.1):A1-18.

[126] Masel J, Genoud N, Aguzzi A. Efficient inhibition of prion replication by PrP-Fc(2) suggests that the prion is a PrP(Sc) oligomer. J Mol Biol. 2005 Feb 4;345(5):1243-51.

[127] Jay R. Silveira, Gregory J. Raymond, Andrew G. Hughson, Richard E. Race, Valerie L. Sim, Stanley F. Hayes& Byron Caughey. The most infectious prion protein particles. Nature. 2005;437:257-261.

[128] Orgel LE. Prion replication and secondary nucleation. Chem Biol. 1996 Jun; 3(6):413-4.

[129] Zrinka Marijanovic, Anna Caputo, Vincenza Campana, and Chiara Zurzolo. Identification of an Intracellular Site of Prion Conversion. PLoS Pathog. 2009 May; 5(5):e1000426.

[130] Godsave SF, Wille H, Kujala P, Latawiec D, DeArmond SJ, Serban A, Prusiner SB, Peters PJ. Cryo-immunogold electron microscopy for prions: toward identification of a conversion site. J Neurosci. 2008 Nov 19;28(47):12489-99.

[131] Hermann C Altmeppen, Berta Puig, Frank Dohler, Dana K Thurm, Clemens Falker, Susanne Krasemann, and Markus Glatzel. Proteolytic processing of the prion protein in health and disease. Am J Neurodegener Dis. 2012;1(1):15-31.

[132] Frederick R. Maxfield& Timothy E. McGraw. Endocytic recycling. Nature Reviews Molecular Cell Biology. 2004 February;5:121-132.

[133] Uchiyama, K., et al. Prions disturb post-Golgi trafficking of membrane proteins. Nat Commun. 2013;4:1846.

[134] Gerber, R., et al. Conformational pH dependence of intermediate states during oligomerization of the human prion protein. Protein Sci. 2008;17(3):537-44.

[135] Schneider, C.A., Rasband, W.S., Eliceiri, K.W. NIH Image to ImageJ: 25 years of image analysis. Nature Methods. 2012;9:671-675.

[136] Tzaban S., Friedlander G., Schonberger O., Horonchik L., Yedidia Y., Shaked G., Gabizon R., Taraboulos A. Protease-sensitive scrapie prion protein in aggregates of heterogeneous sizes. Biochemistry. 2002;41:12868-12875.

[137] Safar J. G., Geschwind M. D., Deering C., Didorenko S., Sattavat M., Sanchez H., Serban A., Vey M., Baron H., Giles K., et al. Diagnosis of human prion disease. Proc. Natl. Acad. Sci. U.S.A. 2005;102:3501-3506.

[138] Pastrana M. A., Sajnani G., Onisko B., Castilla J., Morales R., Soto C., Requena J. R. Isolation and characterization of a proteinase K-sensitive PrP(Sc) fraction. Biochemistry. 2006;45:15710-15717.

[139] Eghiaian, F., et al. Insight into the PrPC -> PrPSc conversion from the structures of antibody-bound ovine prion scrapie-susceptibility variants. Proc Natl Acad Sci U S A. 2004;101(28):10254-10259.

[140] van der Kamp M. W., Daggett V. The consequences of pathogenic mutations to the human prion protein. Protein Eng. Des. Sel. 2009;22;461-468.